Milan J. Math. Vol. 78 (2010) 643–682
DOI 10.1007/s00032-010-0124-5
Published online July 15, 2010

Milan Journal of Mathematics

Reflections on the Lemniscate of Bernoulli: The Forty-Eight Faces of a Mathematical Gem

Joel C. Langer and David A. Singer

Abstract. Thirteen simple closed geodesics are found in the lemniscate. Among these are nine "mirrors"—geodesics of reflection symmetry—which generate the full octahedral group and determine a triangulation of the lemniscate as a *dis-dyakis dodecahedron*. New visualizations of the lemniscate are presented.

Contents

1. Introduction 643
2. Planets, steam engines and airplanes 647
3. The view from the north pole 651
4. Octahedral symmetry 653
5. Mirrors and foci 654
6. Projective symmetries of the lemniscate 658
7. Inversion: quadrics and trinodal quartics 661
8. Triangulation of the lemniscate 664
9. The Riemannian lemniscate 667
Appendix A. Reflections in $\mathbb{R}^3$, $\mathbb{C}^3$ and $\mathbb{C}P^2$ 673
Appendix B. Equivariant parameterization of the quadric 676
Appendix C. Two *Mathematica* animations 680
References 681

1. Introduction

The plane curve known as *the lemniscate of Bernoulli*, which resembles ∞, has played a key role in the history of mathematics (see [15]). Briefly, the *lemniscatic integral* for the curve's arclength was considered by James Bernoulli (1694) in the course of his investigation of thin elastic rods; Count Fagnano (1718) discovered a formula for

"doubling the arc" of the lemniscate, based on the lemniscatic integral; Euler (1751) took the first steps towards extending Fagnano's formula to a more general addition theorem for elliptic integrals. Because it had far-reaching consequences, eventually, Euler's insight was hailed by Jacobi as the birth of the theory of elliptic functions.

Fagnano's doubling formula and his related methods for division of a quadrant of ∞ into two, three, or five equal subarcs by ruler and compass also anticipated developments in algebra and number theory. Gauss (1796) proved constructibility of the 17-gon by ruler and compass, which is equivalent to solving the equation $x^{17} - 1 = 0$ by square roots. He later established that the circle can be divided into n equal parts when $n = 2^j p_1 p_2 \dots p_k$, where the integers $p_i = 2^{2^{m_i}} + 1$ are distinct *Fermat primes*. Apparently inspired by Gauss, Abel (1827) presented a proof of the corresponding result on subdivision of the lemniscate in his treatise on elliptic functions (see [13] and [12]).

The geometry of the lemniscate is not widely known. Recall that the lemniscate may be described by the Cartesian equation $(x^2 + y^2)^2 = A(x^2 - y^2)$; from the polar coordinate equation, $r^2 = A \cos 2\theta$, the qualitative picture ∞ of the real curve follows (for $A > 0$). If we expand our vision of the lemniscate, however, to include *complex* (and infinite) points on the lemniscate, not just the "visible" (real) ones, we can discover the hidden symmetries it possesses.

The full complex curve looks topologically like a sphere; in other words, as a complex algebraic curve, the lemniscate ∞ has *genus zero*. More precisely, it is an immersed copy of the Riemann sphere $S^2 = \mathbb{C}P^1$ in complex projective space $\mathbb{C}P^2$ with three self-intersections. These singularities, known as *nodes* or *double points* (which also happen to be the *inflection points* of ∞), must be permuted by any projective transformation taking ∞ to itself. In [9], the authors prove:

Theorem 1.1. *The subgroup of the projective group $PGL(3, \mathbb{C})$ describing symmetries of the lemniscate is abstractly isomorphic to the (24 element) octahedral group $\mathcal{O}$. Up to projective equivalence, the lemniscate is the unique genus zero curve of degree less than or equal to four with this property.*

The lemniscate may also be characterized as the unique curve in the above class with Riemannian isometry group isomorphic to $\mathcal{O}$; here, isometries are defined via the Fubini-Study metric on $\mathbb{C}P^2$ and are projective transformations represented by unitary matrices.

For a more concrete picture of the complex curve ∞ and its octahedral symmetry, one would like to be able to identify all the familiar features of the octahedron within the lemniscate. To do so, we will use the standard model of the octahedron as a triangulation of the Riemann sphere $x_1^2 + x_2^2 + x_3^2 = 1$: The six vertices are $(\pm 1, 0, 0), (0, \pm 1, 0), (0, 0, \pm 1)$, the twelve edges lie in the three geodesics C_1, C_2, C_3 (great circles) obtained by intersection of the sphere with coordinate planes $x_1 = 0, x_2 = 0, x_3 = 0$, which subdivide the sphere into eight faces (octants).

Meanwhile, since the lemniscate is not quite embedded in $\mathbb{C}P^2$, as a topological copy of S^2, the desired *translation* between sphere and lemniscate will often require

us to identify the latter with its underlying Riemann surface $\mathbb{C}P^1$. In this context, it is helpful to know that the group of symmetries of ∞ may also be viewed intrinsically as a subgroup of the *Möbius group* $PGL(2,\mathbb{C})$, the full group of automorphisms of $\mathbb{C}P^1$.

Thus, to begin the translation, we note that the six octahedral vertices $v_j \in \mathbb{C}P^1$ correspond to the three double points of ∞, as one would expect. This is the easy part! For these points stand out as the only singularities of the lemniscate. To take the next step, we note that the vertices v_j may also be identified, more intrinsically, as the points in $\mathbb{C}P^1$ whose $\mathcal{O}$-orbits have length six. In fact, all but 26 points of $\mathbb{C}P^1$ belong to orbits of length 24 (we'll get to the other exceptional points in a moment). In particular, most edge points "look like" face points from the standpoint of $\mathcal{O}$—which brings us to the question: *How do we unambiguously identify the "octahedral edges" in* ∞*?*

The plane curve $\infty_{\mathbb{R}}$ itself provides the key: As for any real algebraic curve $f(x,y) = 0$, complex conjugation of the Cartesian coordinates x, y defines an anti-holomorphic involution $\mathcal{R}$ of ∞ which fixes the real points $\infty_{\mathbb{R}} = \infty \cap \mathbb{R}P^2$. The *mirror* for this orientation-reversing, reflection symmetry of ∞ is the real (projective) plane $\mathcal{M} = \mathbb{R}P^2 \subset \mathbb{C}P^2$. Turning things around, one could say that the mirror $\mathcal{M}$ determines both the antiholomorphic involution $\mathcal{R}$ and the real one-dimensional curve $\infty_{\mathbb{R}}$.

Returning to the search for octahedral edges, however, it turns out that $\infty_{\mathbb{R}}$ contains, not *four*, but only *two* of the vertices v_j! Namely, we will eventually find that the visible double point of ∞ at the origin corresponds to north and south poles $(0,0,\pm 1) \in S^2$, and $\infty_{\mathbb{R}}$ corresponds to a *fourth* great circle C_4—namely, the one cut out by the plane $x_1 + x_2 = 0$. On the other hand, the reflection of S^2 which fixes C_4 generates, together with $\mathcal{O}$, the full octahedral group $\hat{\mathcal{O}}$; and this group of 48 elements contains *nine* reflection symmetries—including the three reflections in coordinate planes.

The strategy for locating octahedral edges in the lemniscate is now at hand. Let $\mathcal{O}$ act on ∞, and let $\hat{\mathcal{O}}$ be the full group of (holomorphic/antiholomorphic) symmetries generated by $\mathcal{O}$ and $\mathcal{R}$. Then locate the curves in ∞ fixed by the three antiholomorphic reflections $\mathcal{R}_1, \mathcal{R}_2, \mathcal{R}_3 \in \hat{\mathcal{O}}$, each of which fixes four of the points v_j. Each of the resulting curves is subdivided by its four vertices into the desired octahedral edges. Problem solved! (Except for all the details.)

But if the real goal here is to visualize the lemniscate's remarkable structure as fully as possible—which it is—why stop now, at this coarse, octahedral triangulation of the lemniscate? The real lemniscate $\infty_{\mathbb{R}}$ is permuted by $\hat{\mathcal{O}}$ among six curves, each of which is fixed by one of the remaining six antiholomorphic reflections $\mathcal{R} = \mathcal{R}_4, \mathcal{R}_5, \mathcal{R}_6, \mathcal{R}_7, \mathcal{R}_8, \mathcal{R}_9$. The six curves by themselves triangulate ∞ as a *tetrakis hexahedron*, with 24 faces, 36 edges and 14 vertices (see Figure 6). Taken together, the $9 = 3 + 6$ curves of reflection symmetry triangulate ∞ as a *disdyakis dodecahedron*, with 48 faces, 72 edges and $26 = 6 + 8 + 12$ vertices (see Figure 7). In this case the vertices are of three types, formed by the intersection of 4, 3, or 2 of the nine curves. This fine triangulation, whose 48 faces are permuted simply transitively by

$\hat{\mathcal{O}}$, provides the most satisfactory visualization of the lemniscate. Half of the faces are shown in Figure 8, representing one of two sheets of ∞ in *isotropic projection*.

The Riemannian structure alluded to in Theorem 1.1 provides a concise language for carrying the above discussion further. For example, the real lemniscate $\infty_{\mathbb{R}}$ is a simple closed geodesic in the *Riemannian lemniscate*, meaning the underlying Riemann surface $\mathbb{C}P^1$, together with the $\mathcal{O}$-invariant Riemannian metric provided by the theorem.

Theorem 1.2. *The Riemannian lemniscate has (at least)* 13 *simple closed geodesics. There are exactly* 9 *such geodesics of isometric reflection symmetry, and these determine an $\hat{\mathcal{O}}$-invariant triangulation $\mathcal{T} = \cup_{n=1}^{48} \mathcal{T}_n$ of the lemniscate as a disdyakis dodecahedron. Each geodesic triangle T_n has angles $\frac{\pi}{2}, \frac{\pi}{3}, \frac{\pi}{4}$. Reflections $\mathcal{R}_i, \mathcal{R}_j, \mathcal{R}_k$ in the three geodesics bounding T_n generate the full octahedral group $\hat{\mathcal{O}}$, which permutes the triangles of $\mathcal{T}$ simply transitively and defines vertex orbits $\mathcal{V}_6, \mathcal{V}_8, \mathcal{V}_{12}$.*

The latter correspond to the three types of critical points of the lemniscate's Gaussian curvature K: On the six octahedral vertices $\mathcal{V}_6$, $K = K_{max} = 2$; on $\mathcal{V}_8$, $K = K_{min} = -7$; on $\mathcal{V}_{12}$, $K = K_{saddle} = -\frac{1}{4}$. Accordingly, the gradient vectorfield $X = \nabla K$ has critical point index sum: $\chi(S^2) = \sum \mathrm{ind}_X(p) = 6 - 12 + 8 = 2$.

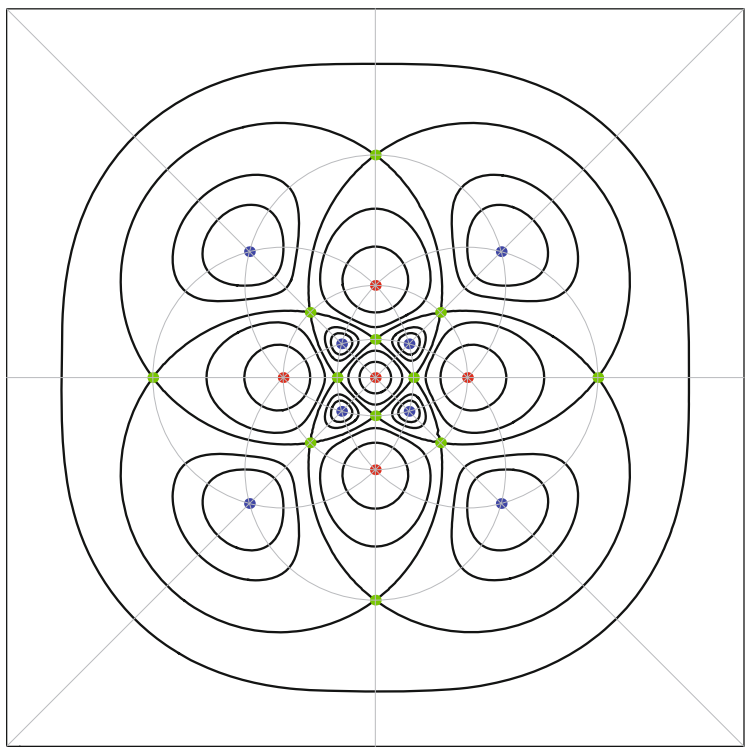

FIGURE 1. Contours and critical points of Gaussian curvature; nine geodesics of reflection symmetry (gray).

One could say, to stretch the point only a little, such a theorem scarcely requires proof. *The Bernoulli lemniscate is what it is, a mathematical gem.* It is also a wonderful excuse for a leisurely tour, in the spirit of mathematical rediscovery, through centuries and diverse branches of science and mathematics. We will return from our excursions with numerous images of the gem, not to mention a veritable menagerie of mappings and groups: Joukowski and spinor maps; stereographic, isotropic and (two) Hopf projections; inversion, Cayley, and Cremona transformations; special linear and projective groups; real and complex orthogonal groups; unitary and extended unitary groups. And yes, a proof. *And yet, by journey's end, we will hardly have scratched the surface of the Bernoulli lemniscate.*

2. Planets, steam engines and airplanes

The lemniscate is often derived geometrically as a special member of the family of plane curves known as *Cassinians* (after the astronomer Cassini considered such curves, in 1680, as candidates for planetary orbits). Fixing numbers $a > c > 0$ and a pair of *foci* $c_\pm = (0, \pm c)$, the Cassinian is the locus of points (x, y) the product of whose distances from $c_\pm$ has the constant value $d_+ d_- = a^2 - c^2$. (The analogy to conics, it will turn out, is more than just that.) The quartic equation of this curve is $(x^2 + (y-c)^2)(x^2 + (y+c)^2) = (a^2 - c^2)^2$, i.e.,

$$f(x, y) = (x^2 + y^2)^2 + 2c^2(x^2 - y^2) = a^2(a^2 - 2c^2).$$

Observe in Figure 2 a) the level sets $f(x, y) = a^2(a^2 - 2c^2)$ belong to one of three cases. For $B = a^2 - 2c^2 < 0$ the level set consists of a pair of smooth curves, each with one focus in its interior; for $B > 0$ the level set is a single smooth curve, which is non-convex as B first turns positive, becoming convex and increasingly round as B increases (say, with c fixed). We are particularly interested in the critical level set $f(x, y) = 0$, the lemniscate resembling 8—henceforth, our lemniscate stands upright! The curve meets the y-axis at $(x, y) = (0, \pm\sqrt{2}c)$ and *twice* at the origin $(0, 0)$. The angle of self-intersection at this double point (node) is 90°; for small values of $r^4 = (x^2 + y^2)^2$, 8 resembles its pair of tangent lines $0 = (x^2 - y^2) = (x - y)(x + y)$.

It is well-known that the lemniscate is *inverse* to a rectangular hyperbola with respect to a circle—see Figure 2 b). Our (non-standard) use of the term derives from complex notation, in which the inverse of a point $z = x + iy$ with respect to the circle $|z|^2 = x^2 + y^2 = c^2$ is given by

$$\sigma(z) = \frac{c^2}{z} = \frac{c^2(x - iy)}{(x^2 + y^2)}, \tag{2.1}$$

with special definitions $\sigma(0) = \infty$, $\sigma(\infty) = 0$. NOTE: We have reason, below, to prefer the term *reflection* for the antiholomorphic map $\rho(z) = \frac{c^2}{\bar{z}}$, standardly called *inversion*!

Inversion $z \mapsto \sigma(z)$ is an involutive transformation ($\sigma(\sigma(z)) = z$) which takes the circle ◯ to itself and interchanges "inside" and "outside". Let ⌒ denote the

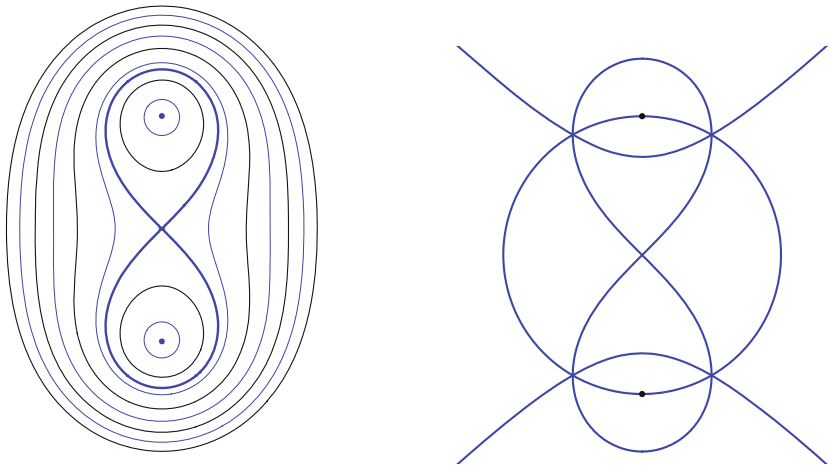

FIGURE 2. a) The lemniscate as Cassinian $d_+d_- = constant$;
b) The trio O)(8: The circle, rectangular hyperbola and lemniscate.

hyperbola with equation $y^2 = x^2 + c^2/2$, and let us rewrite this equation as $0 = Re[z^2] + c^2/2$. Then $z \in \sigma(\smile\!\frown)$ implies $\sigma(z) \in \ \frown\!\smile$, i.e., $0 = Re[\sigma(z)^2] + c^2/2 = c^4\frac{x^2-y^2}{(x^2+y^2)^2} + c^2/2$. Since this is just a rearrangement of the equation for 8, we conclude: $\sigma(\smile\!\frown) = 8$ and $\sigma(8) = \ \frown\!\smile$. Because of the importance of this relationship, we will use "O)(8" as typographical shorthand for the trio of curves in Figure 2 b).

Figure 3 shows a three-rod linkage attributed to James Watt (1784) (see [16]). As the end rods pivot at foci, the middle rod's midpoint traces out 8; thus, the linkage could be thought of as a "lemniscate machine" for draftsmen—though Watt himself had very different applications in mind. He considered a more general linkage, and was especially interested in converting circular motion into linear motion.

We will explain the lemniscate machine as an application of inversion, the focal property of 8 as a Cassinian, and *Joukowski maps*: $j_\pm(z) = \frac{1}{2}(z \pm \frac{1}{z})$. Here we invoke yet another important scientific topic from another century; $j_\pm$ are named after the Russian pioneer of aerodynamics, Nikolai Yegorovich Zhukovsky (1847–1921), who studied airflow around obstacles. Before returning to the lemniscate machine, we will take the time to thoroughly understand the maps $j_\pm$ since they will play an important role in subsequent sections.

First we briefly explain the relevance to applications in 2-dimensional models of fluid flow. Note $j_+(e^{i\theta}) = \cos\theta$, so the unit circle is mapped by j_+ onto the interval $[-1, 1]$, two-to-one except at $z = \pm 1$, where $j_+' = 0$. Since j_+ has degree two and inversion symmetry $j_+(z) = j_+(1/z)$, it follows that the interior and exterior of the unit disc each get mapped conformally onto the slit-plane $\mathbb{C}\setminus[-1, 1]$. Using the latter mapping, the trivial flow to the right given by the constant velocity field $\frac{dz}{dt} = \mathbf{c\hat{i}}$, say, is transformed to *ideal* (incompressible and irrotational) flow around a circular obstacle.

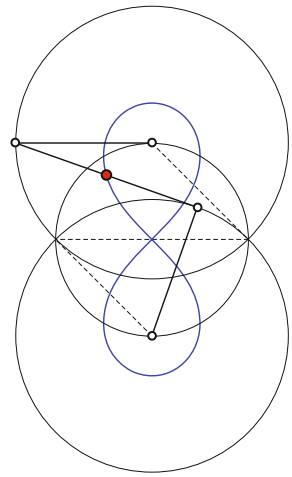

FIGURE 3. The lemniscate machine: The middle rod's midpoint traces out 8.

To build on this, one may then consider more complicated obstacles obtained as j_+-images of other circles—see Figure 4. (One can get a much better feel for the full variety of circle images by running the simple *Mathematica* animation in the Appendix.) One may verify, e.g., that circles $|z| = r_0$ and rays $arg(z) = \theta_0$ are mapped to orthogonal, confocal families of ellipses and hyperbolas with foci ± 1. More to the point, for the Joukowski model of airflow around a wing, circles passing through exactly one of the two points ± 1 are taken to cusped curves resembling airfoils; as a conformal mapping of exteriors, j_+^{-1} transforms ideal flow around the circle to ideal flow around such an airfoil.

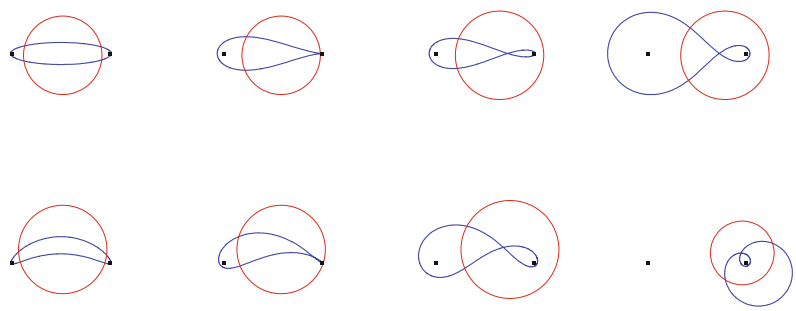

FIGURE 4. Circles C and their Joukowski images $j_+(C)$.

To better understand $j_\pm$, we consider two auxiliary mappings defined by linear fractional transformations:

$$h(z) = \frac{z+1}{z-1}, \quad k(z) = h(iz) = \frac{z-i}{z+i} \tag{2.2}$$

Like any Möbius transformation, h and k map circles to circles. In particular, h (k) maps circles through $z = 1$ ($z = -i$) to lines ("circles through ∞"); circles through the pair $z = \pm 1$ ($z = \pm i$) are mapped to lines through the origin. We note that the *Cayley map* $k(z)$ restricts to a conformal map of the upper half-plane $H = \{z = x + iy : \ y > 0\}$ onto the unit disc $D = \{z = x + iy : \ x^2 + y^2 < 1\}$. (The important equivalence $k : H \to D$ explains why $k(z)$ deserves a name.) Likewise, $h(z)$ maps a half-plane ($Re[z] < 0$) to the unit disc. But there is an interesting difference between the two maps: h is its own inverse, i.e., h has *order two*, while $k(z)$ has *order three* (more on this later).

Returning to the Joukowski maps, we find that $j_\pm$ may be understood as the squaring function $z \mapsto z^2$, conjugated by h or k:

$$\begin{aligned} j_+(z) &= \frac{1}{2}(z + \frac{1}{z}) = h(h(z)^2) = j_+(1/z) \\ j_-(z) &= \frac{1}{2}(z - \frac{1}{z}) = k^{-1}(k(z)^2) = j_-(-1/z) \end{aligned}$$

Here we have also recorded the respective symmetries $z \mapsto \pm 1/z$ of these two-to-one maps inherited from the symmetry $z^2 = (-z)^2$; the points $0, \infty$, which are both fixed points and points of ramification ("wrapping") for $z \mapsto z^2$, are replaced by ± 1 for j_+ and $\pm i$ for j_-.

Certain mapping properties of $j_\pm$ may now be easily understood. For instance, since h exchanges circles through ± 1 with lines through the origin, and $z \mapsto z^2$ "folds" the latter in half, it follows that j_+ maps circular arcs joining ± 1 onto arcs in the same family. Explicitly, a circle through ± 1 is divided by these points into upper and lower arcs $\mathcal{A}_\pm$, with equations of the form $\arg(h(z)) = \theta_0$ and $\arg(h(z)) = \theta_0 + \pi$. The two arcs are *inverse* to each other: $\mathcal{A}_+ = 1/\mathcal{A}_-$. With $w = j_+(z)$, the identity $h(w) = h(z)^2$ implies the images $j_+(\mathcal{A}_\pm)$ satisfy equivalent conditions: $\arg(h(w)) = 2\theta_0$ and $\arg(h(w)) = 2\theta_0 + 2\pi$.

Finally, we return to the lemniscate machine. Let $C_\pm$ be the circles with centers $\pm i$ and radius $\sqrt{2}$. Then j_+ maps C_+ (C_-) onto the upper (lower) half of C, the unit circle $|z| = 1$. If $z \in C_+$, say, then $(j_-(z) - i)(j_-(z) + i) = j_-(z)^2 + 1 = j_+(z)^2 \in C$, and it follows that $w = j_-(z)$ lies on the lemniscate (special Cassinian) $d(w, i)d(w, -i) = 1$. Further, $z \in C_+ \Rightarrow 1/z \in C_+ \Rightarrow -1/z \in C_-$. Now the line segment ("middle rod") joining $z \in C_+$ to $-1/z \in C_-$ has constant length $|z + 1/z| = 2|j_+(z)| = 2$, while its midpoint $j_-(z)$ lies on the lemniscate.

Suppose a motor rotates the upper rod with constant angular speed $\frac{d\theta}{dt} = 1$. Then the motions of the middle rod's endpoints (on $C_\pm$) and midpoint (on 8) are given by:

$$\begin{aligned} c_+(t) &= \sqrt{2}e^{it} + i, \quad c_-(t) = -1/c_+(t), \\ j_-(c_+(t)) &= \frac{1}{2}(\sqrt{2}e^{it} + i - 1/(\sqrt{2}e^{it} + i)) \end{aligned}$$

This is the basis of the *Mathematica animation* of the lemniscate machine in the Appendix.

3. The view from the north pole

Armed with an understanding of the Joukowski maps $j_\pm$, we are within steps of startling new views of the trio of curves O)(8. As we have just seen, $j_-(C_+) = 8$; therefore, $j_-(C_-) = j_-(-1/C_+) = 8$ as well. Likewise, the two lines $x \pm y = 0$ are exchanged by $z \mapsto -1/z$, and each is mapped by j_- onto the rectangular hyperbola $\frown\!\!\!\!\smile$. Finally, $j_+(C_\pm) = C$, so $j_-(iC_\pm) = -ij_+(-C_\pm) = C$ as well. However, iC_+, iC_- are preserved, not exchanged, by $z \mapsto -1/z$; that is, points $\pm i$ divide iC_+ into left/right arcs which are exchanged by $z \mapsto -1/z$ (and likewise for iC_-). Thus, C is double-covered by a pair of "folded circles" $j_-(iC_\pm)$ meeting at foci $\pm i$.

Putting all the pieces together, we see that O)(8 is the two-to-one image under j_- of the symmetric configuration of six circles/lines shown in Figure 5 a)—which we denote, henceforth, by $\mathcal{C}_6$. The symmetry of $\mathcal{C}_6$ may be taken as a clue to the high degree of symmetry of the lemniscate itself, but a full explanation will require further background. In the meantime, we consider the geometric meaning of $\mathcal{C}_6$ itself, and seek further clues to its relationship with 8.

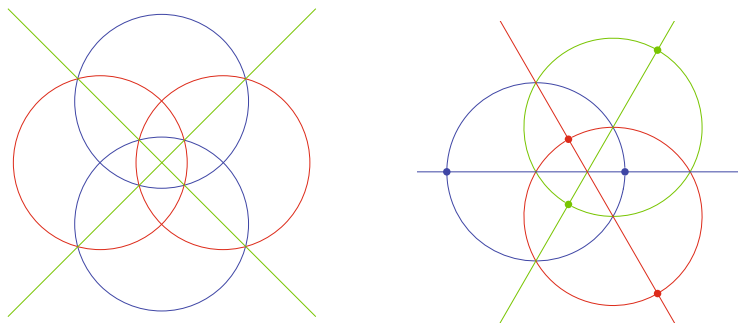

FIGURE 5. a) $\mathcal{C}_6$ is mapped by $j_-(z)$, *two-to-one* onto O)(8.
b) A Möbius equivalent figure $m(\mathcal{C}_6)$.

$\mathcal{C}_6$ has obvious fourfold rotational symmetry. But there is also an order *three* symmetry, apparent in the Möbius equivalent Figure 5 b) (obtained by sending an appropriate pair of threefold intersection points to the origin and infinity). If one steps outside the Euclidean plane, in fact, both symmetries may be regarded as rotational symmetries of the *same figure*.

All that is required is to place the configuration of circles on the standard unit sphere $x_1^2 + x_2^2 + x_3^2 = 1$ using *stereographic projection from the north pole*:

$$(x_1, x_2, x_3) \overset{\pi}{\longmapsto} \zeta = \frac{x_1 + ix_2}{1 - x_3} \tag{3.1}$$

$$\zeta = u + iv \overset{\pi^{-1}}{\longmapsto} (x_1, x_2, x_3) = \left(\frac{2u}{u^2+v^2+1}, \frac{2v}{u^2+v^2+1}, \frac{u^2+v^2-1}{u^2+v^2+1} \right) \tag{3.2}$$

To fit with complex notation, we have identified the equatorial x_1, x_2-plane with the complex plane via $(x_1, x_2) \leftrightarrow \zeta = x_1 + ix_2$. With this understanding, the projected point $\pi(x_1, x_2, x_3)$ is pictured as the intersection of the equatorial plane with the line through the north pole $(0, 0, 1)$ and (x_1, x_2, x_3). An important feature of the construction is that π^{-1} has well-defined limit at infinity, $\lim_{\zeta\to\infty} \pi^{-1}(\zeta) = (0, 0, 1)$, and putting $\pi(0, 0, 1) = \infty$ extends π to a smooth bijection between the whole *Riemann sphere* and the extended complex plane $\hat{\mathbb{C}} = \mathbb{C} \cup \{\infty\}$. As explained in any complex analysis textbook, π has the following additional nice properties: π is *conformal* (angle-preserving), and maps a circle C on the Riemann sphere to a line or circle in $\mathbb{C}$, depending on whether C contains the north pole or not.

Of course, there is nothing sacred about the north pole in this geometric construction; for instance, in place of $\pi = \pi_{np}$, we could use projection π_{sp} from the south pole $(0, 0, -1)$ onto the equatorial plane, obtained by simply changing '$-$' to '$+$' in the above formula for π. (For π_{sp}^{-1}, change sign of the third component of π^{-1}.) For that matter, one could project from any "pole" $p \in S^2$ onto the plane P through the origin, normal to the unit vector $\hat{p}$; such a projection is conjugate to π by a rotation of 3-space.

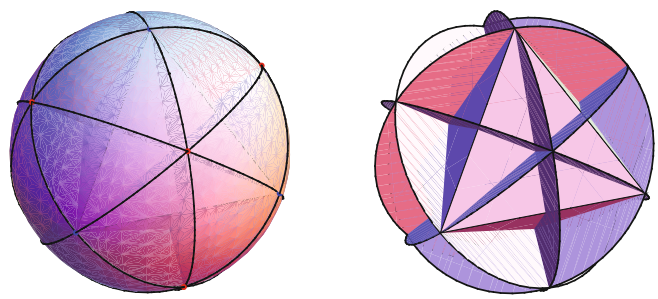

FIGURE 6. a) The (spherical) tetrakis hexahedron $\mathcal{G}_6 = \pi^{-1}(\mathcal{C}_6)$.
b) Octahedron in tetrakis hexahedron.

Now comes the payoff: Using the fact that three points determine a circle, one can verify that $\mathcal{C}_6$ is the π-image of the configuration $\mathcal{G}_6$ of the six *geodesics* (*great circles*) shown in Figure 6 a), b)—and the full symmetry leaps off the page! In fact, $\mathcal{G}_6$ may be regarded as a (spherical) *tetrakis hexahedron*, whose vertices, edges, and faces satisfy *Euler's formula*, $\chi(S^2) = V - E + F = 14 - 36 + 24 = 2$. (For counting, $\mathcal{G}_6$ may be viewed as the first barycentric subdivision of a tetrahedron, so $V = VT + ET + FT = 4 + 6 + 4, E = 2ET + 6FT = 12 + 24, F = 6FT = 24$.) Figure 6 b) shows $\mathcal{G}_6$ together with its inscribed octahedron, as visual proof of the octahedral symmetry of $\mathcal{G}_6$.

Before we embark on a more systematic investigation of octahedral symmetry, let us pause to take stock of the relationships we have uncovered so far. We began by noting that the lemniscate may be obtained by inversion of a hyperbola in the unit circle. The trio O)(8 of curves just mentioned was seen to be the *shadow* (projected image) of $\mathcal{C}_6$, which is itself the shadow of $\mathcal{G}_6$, that is:

$$O)(8 = j_-(\mathcal{C}_6) = j_-(\pi(\mathcal{G}_6))$$

Now let us focus on the three circles meeting at a point $P \in S^2$ in the foreground of Figure 6 a), b). Note $p = \pi(P)$ is the threefold intersection of line/circles to the upper right of Figure 5 a), and $j_-(p)$ is the point to the upper right of Figure 2 b) where lemniscate, circle, and hyperbola meet. In all three figures, the local picture is that of six curvilinear sectors with angular measure 60°. Since the three circles meeting at P in Figure 6 are cyclically permuted by rotation of the sphere by 120° about the *axis* $\pm(1,1,1)$, it is tempting to suppose that the roles of the three curves in O)(8 are entirely symmetric: *Might the circle, lemniscate and hyperbola be three coequal partners, each of which may be recovered from the other two?*

4. Octahedral symmetry

Consider first the *standard octahedron* $O = \mathcal{G}_3$ with vertices:

$$\hat{\mathbf{i}} = (1,0,0),\ \hat{\mathbf{j}} = (0,1,0),\ \hat{\mathbf{k}} = (0,0,1),$$

and antipodes $-\hat{\mathbf{i}},\ -\hat{\mathbf{j}},\ -\hat{\mathbf{k}}$. Using the basis $\hat{\mathbf{i}},\ \hat{\mathbf{j}},\ \hat{\mathbf{k}}$, the 24-element octahedral symmetry group $\mathcal{O}$ is represented by the 3×3 matrices with determinant *one* and exactly *three* non-zero entries, $a_{mn} = \pm1$. The elements of $\mathcal{O}$ permute the edges of $\mathcal{G}_3$; any vertex may be taken to any other and, fixing one vertex, the four adjacent vertices may be (cyclically) permuted.

To enumerate all (non-identity) elements of $\mathcal{O}$, there are: 6 elements of order *four* (rotations by $\pi/4$ or $3\pi/4$ about x_1, x_2, x_3 coordinate axes; 8 elements of order *three* (rotations by $2\pi/3$ or $4\pi/3$ about "dual-cube diagonals" $\pm(1,1,1)$, $\pm(-1,1,1)$, $\pm(1,-1,1)$, $\pm(1,1,-1)$); $9 = 3 + 6$ elements of order *two* (rotations by π about coordinate axes or about axes joining midpoints of opposite edges). The $24 = 1 + 6+8+3+6$ elements are grouped by this description into *five* conjugacy classes; two equivalent elements a and $b^{-1}ab$ play essentially the same role, not just as elements of an abstract group $\mathcal{O}$, but as symmetries of $\mathcal{G}_3$ or $\mathcal{G}_6$.

As our notation $O = \mathcal{G}_3$ suggests, the octahedron may be viewed as a configuration of 3 geodesics (intersections of the sphere with coordinate planes), which complement the six geodesics of $\mathcal{G}_6$. It is easy to see that $\mathcal{G}_3$ and $\mathcal{G}_6$ have the same symmetry groups by considering vertices of the two polyhedra. In fact, $\mathcal{G}_6$ has the 6 vertices of $\mathcal{G}_3$, together with the 8 "dual vertices" $(\pm1,\pm1,\pm1)/\sqrt{3}$; a rotation permuting the first 6 vertices automatically permutes the dual vertices.

As an abstract group, $\mathcal{O}$ is solvable, with normal series $1 \lhd V \lhd T \lhd \mathcal{O}$. The abelian subgroup V known as the *Klein four group* consists of the identity 1 and the three 180°-rotations about coordinate axes. The normal subgroup T may be

described as the 12-element symmetry group of either of two associated tetrahedra; namely, the *stellated octahedron* may be thought of as a dual pair of regular tetrahedra, whose intersection gives the edges and vertices of the octahedron itself. Whereas the tetrahedral group T takes each associated tetrahedron to itself, $\mathcal{O}$ may also "swap" the two. It is also useful to compare the descriptions of $\mathcal{O}$ and T by generators and relations: $\mathcal{O} = \langle a, b \mid a^2 = b^3 = (ab)^4 = 1\rangle$, while the tetrahedron lacks symmetries of order *four* and is given by $T = \langle a', b \mid a'^2 = b^3 = (a'b)^3 = 1\rangle$. Here, $a' \in V$, and $a \in \mathcal{O}$ is an order *two* element which swaps tetrahedra (and fixes no vertex or face of O).

As abstract groups, $\mathcal{O}$ and T are often identified, respectively, with the *symmetric* and *alternating groups on four letters* S_4 and A_4. (To interpret $\mathcal{O} \simeq S_4$, we note that the elements of $\mathcal{O}$ arbitrarily permute the above-mentioned diagonals of the dual cube.) The fact that S_4 is solvable is directly associated with the solvability by radicals of quartic polynomial equations. Explicit procedures for solving cubics and quartics make use of the key substitution $2w = z + \frac{1}{z}$—small world!

Now we return to the configuration of circles and lines $\mathcal{C}_6$. Note that π maps the six octahedral vertices, ± 1, $\pm i$, 0, ∞, to the points of twofold intersection in $\mathcal{C}_6$, and the 8 dual vertices to the threefold intersections. In terms of the Riemann sphere parameter $\zeta = \pi(x_1, x_2, x_3)$, the 24 "octahedral symmetries" of $\mathcal{C}_6$ are given by the following Möbius transformations $w = m(\zeta)$:

$$\zeta \longmapsto i^n\zeta,\ \frac{i^n}{\zeta},\ i^n h(\zeta),\ \frac{i^n}{h(\zeta)},\ i^n k(\zeta),\ \frac{i^n}{k(\zeta)},\ n = 0, 1, 2, 3. \tag{4.1}$$

For example, the Cayley map $k(\zeta) = \frac{\zeta - i}{\zeta + i}$ satisfies $k(-i) = \infty,\ k(\infty) = 1,\ k(1) = -i$, and corresponds to rotation by 120° about the axis through the pair of dual vertices $\pm(1, -1, 1)/\sqrt{3}$; in particular, $k(\zeta)$ cyclically permutes pre-images of the three curves in O)(8. Likewise, $h(\zeta) = \frac{\zeta + 1}{\zeta - 1}$ corresponds to rotation by 180° about the axis through $\pm(1, 0, 1)/\sqrt{2}$. Together, the two transformations $h(\zeta),\ k(\zeta)$ generate the whole group of 24 symmetries.

5. Mirrors and foci

Of the many objects possessing octahedral symmetry, we have thus far concentrated on the octahedron $\mathcal{G}_3$ and the tetrakis hexahedron $\mathcal{G}_6$. In the present section we indicate the important role of the *disdyakis dodecahedron*—see Figure 7a)—which is determined by the 9 geodesics $\mathcal{G}_9 = \mathcal{G}_3 \cup \mathcal{G}_6$. As is the case for $\mathcal{G}_3$ and $\mathcal{G}_6$, the vertices of the spherical polyhedron $\mathcal{G}_9$ are the points of intersection of the geodesics, and the edges are the geodesic arcs between consecutive intersections. The intersection $\mathcal{G}_3 \cap \mathcal{G}_6$ adds 12 new vertices (midpoints of octahedral edges) to those of $\mathcal{G}_3$ and $\mathcal{G}_6$, giving $\mathcal{G}_9$ a total of $26 = 6 + 8 + 12$ vertices, of three types. The latter subdivide each geodesic of $\mathcal{G}_9$ into eight parts, and Euler's formula reads $\chi = 26 - 72 + 48 = 2$. (These numbers also follow by viewing $\mathcal{G}_9$ as the first barycentric subdivision of an octahedron.)

We have limited ourselves, till now, to symmetries given by rotations of S^2; but it is natural to consider also the orientation-reversing symmetries determined by geodesics. A given geodesic is the intersection of the sphere $S^2 \subset \mathbb{R}^3$ with a plane $\mathcal{P}$ through the origin, and reflection of points across the "mirror" $\mathcal{P}$ restricts to the associated *reflection symmetry* of S^2. Let $\mathcal{G}$ be the space of all geodesics in S^2—note this is the projective plane $\mathcal{G} \simeq \mathbb{R}P^2$. Denote by $R(\mathcal{G})$ the group generated by all reflections in geodesics and let $R_2(\mathcal{G})$ be the subgroup generated by pairs of such reflections (applied iteratively). We note that $R(\mathcal{G})$ is the orthogonal group $O(3)$, and $R_2(\mathcal{G}) = SO(3)$; in fact, any rotation is a product of two reflections and any orthogonal transformation is a product of at most three reflections. Such conclusions follow easily from the following basic fact: If $\mathcal{P}_1$ and $\mathcal{P}_2$ are two planes through the origin with line of intersection L and forming dihedral angle θ, then consecutive reflections in $\mathcal{P}_1$, $\mathcal{P}_2$ produce a rotation by angle 2θ with axis L.

Now if $R(\mathcal{G}_N)$ and $R_2(\mathcal{G}_N) = R(\mathcal{G}_N) \cap SO(3)$ denote the corresponding groups generated by reflecting only in the geodesics belonging to $\mathcal{G}_N$, then the three cases yield familiar finite groups—the Klein four group, tetrahedral and octahedral groups:

$$R_2(\mathcal{G}_3) = V, \quad R_2(\mathcal{G}_6) = T = \mathcal{A}_4, \quad R_2(\mathcal{G}_9) = \mathcal{O} = S_4$$

The last of these equations is the most important for us. One may consider the three geodesics G_1, G_2, G_3 bounding a given face F_0 of $\mathcal{G}_9$, and observe that all faces of $\mathcal{G}_9$ lie in the orbit of F_0 under the group generated by reflections in G_1, G_2, G_3. One may thus convince oneself that $\mathcal{G}_9$ generates the *full octahedral group* $\hat{\mathcal{O}} = R(\mathcal{G}_9)$, and that this 48-element group acts simply transitively on faces of $\mathcal{G}_9$. Note that the "checkerboard" coloring in Figure 7a) is helpful for distinguishing $\mathcal{O}$ from $\hat{\mathcal{O}}$ symmetries: An even number of reflections preserves the color of a tile, and the 48 tiles are divided into two color-coded $\mathcal{O}$-orbits.

As the previous paragraph suggests, the disdyakis dodecahedron exhibits octahedral symmetry more satisfactorily than any other polyhedron. The assertion is amplified by consideration of orbits of points $p \in S^2$. First, the (three types of) vertices of $\mathcal{G}_9$ are distinguished by having $\mathcal{O}$-orbits of length $6, 8$, or 12; any other point belongs to an orbit of length 24. Expanding to the full octahedral group $\hat{\mathcal{O}}$ yields orbit lengths: $6, 8, 12, 24, 48$. While the orbit of a *face point* has thus doubled in length, the orbit of an *edge point* is unchanged, since it is fixed by reflection in its geodesic. To summarize, the sets of vertices, edge points and face points of the disdyakis dodecahedron $p \in \mathcal{G}_9 \approx S^2$ are characterized by their $\hat{\mathcal{O}}$-orbit lengths $|p| = |\hat{\mathcal{O}} \cdot p|$ as follows:

$$\mathcal{V} = \{p : |p| \in \{6, 8, 12\}\}, \quad \mathcal{E} = \{p : |p| = 24\}, \quad \mathcal{F} = \{p : |p| = 48\} \tag{5.1}$$

It is interesting to view reflections in a slightly different context, where the "mirrors" are no longer planes. Instead of the metric sphere $S^2 \subset \mathbb{R}^3$, consider the Riemann sphere or extended complex plane $\hat{\mathbb{C}}$. Then reflection in the real line is given by complex conjugation $z \leftrightarrow \bar{z}$, while reflection in the unit circle "mirror" is given by:

$$z \mapsto z^* = \rho(z) = 1/\bar{z} \tag{5.2}$$

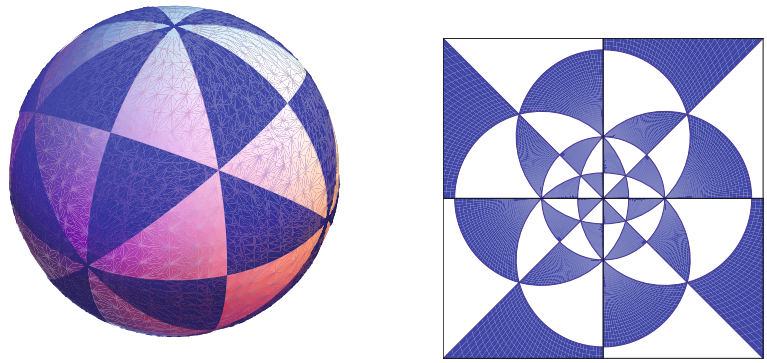

FIGURE 7. *a) Disdyakis dodecahedron $\mathcal{G}_9$; b) Stereographic image $\pi(\mathcal{G}_9)$.*

(The polar coordinate formula $(r,\theta) \overset{\rho}{\longmapsto} (1/r,\theta)$ shows that reflection ρ actually has a simpler geometric meaning than inversion σ.) More generally, letting $\mathcal{C}$ be the space of all circles in the Riemann sphere, we may reflect in any circle $C \in \mathcal{C}$: There exists a unique anti-holomorphic involution $R_C : \hat{\mathbb{C}} \to \hat{\mathbb{C}}$ which fixes points of C.

Now let $R_2(\mathcal{C})$ $(R(\mathcal{C}))$ be the group generated by pairs of (any number of) reflections in circles. It is well-known that one thus obtains the group of Möbius transformations $PSL(2,\mathbb{C}) = R_2(\mathcal{C})$ ($R(\mathcal{C})$ includes all anti-automorphisms of $\hat{\mathbb{C}}$ as well); in fact, any $m \in PSL(2,\mathbb{C})$ may be expressed as a product of (at most) four reflections. We write $R_2(C_N)$ for the corresponding finite subgroups of the Möbius group generated by reflections in pairs of circles of C_3, C_6 or $C_9 = C_3 \cup C_6$. The groups $R(C_9) \simeq \hat{\mathcal{O}}$ and $R_2(C_9) \simeq \mathcal{O}$ may be visualized using Figure 7b), which shows the stereographic image of the disdyakis dodecahedron.

This section began with circles playing a passive role, as objects on which symmetries act. There is also an active role for circles, as the previous paragraphs suggest, and this leads to a concise language for describing symmetries. One may *multiply* circles by letting $A \cdot B = C$ be the circle obtained by reflecting the points of B in A; by this (non-commutative, non-associative) multiplication, $(\mathcal{C},\cdot)$ becomes a three-dimensional *manifold with multiplication*, satisfying the symmetric space axioms (as developed in [10]). The *group of displacements* $G(\mathcal{C})$ is the group of symmetries (automorphisms) of $(\mathcal{C},\cdot)$ generated by pairs of *left multiplications*, $C \mapsto L_A L_B C = A\cdot(B\cdot C)$. Then $G(\mathcal{C}) \simeq PSL(2,\mathbb{C})$; the fact that displacements generate all symmetries (in the component of the identity) is a nice feature of $\mathcal{C}$, shared by other *semi-simple* symmetric spaces. Likewise, the symmetric subspace of great circles $\mathcal{C} \supset \mathcal{G} \simeq \mathbb{R}P^2$ is semi-simple and satisfies the corresponding property $G(\mathcal{G}) \simeq SO(3)$.

Given finitely many circles in $\mathcal{C}$, one may always generate a (countable) symmetric subspace of $(\mathcal{C},\cdot)$; the theory of such examples is very rich (considering that it includes, e.g., the theory of *quasicircles*). But one may check that C_3, C_6 and C_9 are already closed under multiplication; and though their automorphism groups are

all the same ($Aut(C_N) = \hat{\mathcal{O}}$), their displacement groups are not:

$$G(C_3) \simeq \{Id\}, \quad G(C_6) \simeq T, \quad G(C_9) \simeq \mathcal{O}.$$

The above notation suggests an interesting generalization. Let C_1, C_2, C_3 be the three great circles meeting at $P \in S^2$ in the foreground of Figure 6 a), b) (or the three line/circles meeting at $p = \pi(P)$ to the upper right of Figure 5 a)) and observe: $C_1 \cdot C_2 = C_3$, $C_2 \cdot C_3 = C_1$, $C_3 \cdot C_1 = C_2$. (Order of multiplication does not matter in this case.) Comparing the latter circle configurations again with Figure 2 b), it is now tempting to ask if one can give similar meaning to the following equations:

$$\bigcirc \cdot \asymp = 8, \quad \asymp \cdot 8 = \bigcirc, \quad 8 \cdot \bigcirc = \asymp$$

Actually, the first of these equations follows from $\sigma(\asymp) = 8$, since $\asymp$ and 8 happen to be symmetric with respect to the real axis. The other two equations involve "multiplication" by the curves $\asymp$ and 8, which requires the notion of *Schwarzian reflection* R_A in an analytic curve A. The operation R_A generalizes the reflection already defined for circles: R_A is defined, locally, as the antiholomorphic involution fixing points of A.

Such a reflection may be expressed more explicitly as $R_A(z) = \overline{A(z)}$, where $A(z)$ is the *Schwarz function* of A. As developed in [4], $A(z)$ is the holomorphic function defined near A whose restriction to A satisfies $\bar{z} = A(z)$. In the case of an algebraic curve $f(x, y) = g(z, w) = 0$, the Schwarz function is the algebraic function $w = A(z)$ defined by $g(z, w) = 0$; here, g is the polynomial obtained from f by change of variables to *conjugate coordinates* $z = x + iy$, $w = x - iy$ (which play an important role below). Given curves A, B, multiplication $A \cdot B$ gives a new curve C with Schwarz function $C(z) = A \circ B^{-1} \circ A(z)$. This locally defined multiplication may be regarded as a formal symmetric space structure on analytic curves (see [3]).

The Schwarz functions for the unit circle, rectangular hyperbola and lemniscate may be found by solving for w in their respective equations $g(z, w) = 0$:

$$\bigcirc(z) = \frac{1}{z}, \quad \asymp(z) = i\sqrt{1 + z^2}, \quad 8(z) = \frac{iz}{\sqrt{1 + z^2}}$$

One may put these expressions into the formula $C(z) = A \circ B^{-1} \circ A(z)$ and verify the above multiplication table for the three curves—modulo the usual sign ambiguity of square roots. As for any real algebraic curve (other than a circle or line), the Schwarz functions $\asymp(z)$, $8(z)$ are multi-valued in the large; what's unusual, here, is that the two values differ only in sign. Because of this, and the symmetry of the three curves, $z \mapsto -z$, Schwarz reflections $R_{\bigcirc}$, $R_{\asymp}$, R_8 give back only the same curves. (But one could say each curve has been "doubled" in the process, much as the trio $O)(8 = j_-(\mathcal{C}_6)$ is double covered by C_6.)

Finally, we note the special role of the pair of points $\pm i$ in the figure $O)(8$, as branch points of Schwarz functions $\asymp(z)$, $8(z)$ and reflections $R_{\asymp}(z)$, $R_8(z)$. For the purpose of discussing symmetry of the lemniscate, we ultimately choose to work with *planar mirrors*; so we may avoid multi-valued functions and branches associated with "algebraic mirrors". But the branch points themselves are significant geometric features of the hyperbola and lemniscate—these points are the *foci*.

We remark that the sum, difference and product of distances to foci are constant for the respective cases of ellipses, hyperbolas and Cassinians; yet the general definition of focus of a real algebraic curve belongs to the setting of projective geometry and makes no reference to distances at all. (Some basic notions of projective geometry will be reviewed briefly, below.) In the present context, here are the relevant facts (see [8]):

1) The (real) foci of a real algebraic curve A may be described as the singularities of the Schwarz function $A(z)$.

2) Inversion $z \mapsto \sigma(z) = 1/z$ sends foci of A to foci of $\sigma(A)$.

Thus, it is no coincidence that the foci of $\smile$ and $8 = \sigma(\smile)$ coincide!

6. Projective symmetries of the lemniscate

The lemniscate $0 = f(x,y) = (x^2+y^2)^2 + 2c^2(x^2-y^2)$ has "reflection symmetries" $f(-x,y) = f(x,-y) = f(x,y)$ apparent in the real x,y-plane; but these will be seen as *half-turns* when 8 is viewed as a complex curve. Likewise, the identity $f(iy,ix) = f(x,y)$ is a "hidden symmetry" when 8 is viewed in $\mathbb{R}^2$, but a *quarter-turn* for the complex curve.

More hidden is the "non-linear symmetry" $f(x',y') = c^4 f(x,y)/(x-iy)^4$, where $x' = c\frac{c+x+iy}{2(x-iy)}$ and $y' = c\frac{c-x-iy}{2i(x-iy)}$. This identity shows that $f(x',y') = 0$ holds for finite (x',y') $(x \neq iy)$, provided $f(x,y) = 0$. This order-three symmetry, together with one of the above even-order symmetries, generates a transformation group abstractly isomorphic to the octahedral group—but one should not waste the time to verify this! It is evident that our study of symmetry of the lemniscate will require not only *complex points* $(x,y) \in \mathbb{C}^2$, but also the *ideal points* of 8 to be included, and treated on an equal footing; that is, our discussion truly belongs to the setting of complex algebraic curves in complex projective space $\mathbb{C}P^2$. Here, everything will become clearer.

We recall the projective plane is built from the ordinary (affine) plane by adding ideal points ("points at infinity") where parallel lines meet. We describe a point in the projective plane by homogeneous coordinates $[x,y,z] \neq [0,0,0]$, where $[x,y,z] \sim [(\lambda x, \lambda y, \lambda z)]$ for any $\lambda \neq 0$. A point (x,y) in the plane corresponds to the point with projective coordinates $[x,y,1]$. The ideal points are those whose third coordinate is 0. We will allow the coordinates to be complex numbers. An invertible linear transformation of $\mathbb{C}^3$ induces a transformation of $\mathbb{C}P^2$; the group of such transformations is the projective group $P = PGL(3,\mathbb{C})$. It is convenient to represent an element of P as a matrix, with the understanding that any scalar multiple of the matrix represents the same element.

A polynomial equation $f(x,y) = 0$ of degree n defining a plane curve is extended to $\mathbb{C}P^2$ by defining the homogeneous polynomial $F[x,y,z] = z^n f(x/z, y/z)$. With complex points and ideal points included in the solution set, a closed surface is defined by the equation $0 = F[x,y,z]$. For example, a circle $(x-a)^2+(y-b)^2-r^2 = 0$ is extended to $\mathbb{C}P^2$ by the equation $(x-az)^2 + (y-bz)^2 - r^2z^2 = 0$. We note that

any circle thus passes through the *circular points* $\mathcal{I} = [1, -i, 0]$ and $\mathcal{J} = [1, i, 0]$, whose inclusion will allow us to identify the circle with the Riemann sphere.

In the case of the lemniscate, the resulting equation is

$$0 = F(x, y, z) = z^4 f(x/z, y/z) = (x^2 + y^2)^2 + 2c^2 z^2 (x^2 - y^2) \tag{6.1}$$

This curve is a *bicircular quartic*, so called because it has a double point ("node") at each circular point. As it also has a node at the origin $\mathcal{K} = [0, 0, 1]$, the lemniscate is an example of a *trinodal quartic*.

Like a circle, 8 is topologically equivalent to a sphere. The identification of an algebraic curve with the Riemann sphere $\hat{\mathbb{C}}$ is in fact accomplished, once a rational parameterization of the curve is known. For example, the circle $x^2 + y^2 - r^2 z^2 = 0$ has parameterization $x(t) = r(t^2 - 1),\ y(t) = 2rt,\ z(t) = t^2 + 1$, which maps $\hat{\mathbb{C}}$ *one-to-one* onto the circle in $\mathbb{C}P^2$. The lemniscate has parameterization

$$x(t) = \sqrt{2}c(t^3 - t), \quad y(t) = \sqrt{2}c(t^3 + t), \quad z(t) = t^4 + 1 \tag{6.2}$$

Each double point $\mathcal{I}, \mathcal{J}, \mathcal{K}$ is the image of a *pair* of t-values, respectively, $t = \pm e^{i\pi/4}$, $t = \pm e^{i3\pi/4}$, and $t = 0, \infty$. For example, the two "copies" of the origin $\mathcal{K}_0, \mathcal{K}_\infty$ locate the crossing of two *branches*, on each of which t defines a valid local coordinate near $\mathcal{K}_0$ or $\mathcal{K}_\infty$; thus, from an intrinsic point of view, 8 may also be regarded as a copy of $\hat{\mathbb{C}}$. (More generally, the *Uniformization Theorem* enables one to identify any irreducible algebraic curve with a compact Riemann surface of some genus $g \geq 0$, but the situation for $g > 0$ is much more complicated because there are many Riemann surfaces with a given positive genus.)

Now let us return to the issue of symmetry. As a Riemann surface, a genus zero curve $\mathcal{A}$ such as 8 always has the Möbius group $PGL(2, \mathbb{C}) = Aut(\hat{\mathbb{C}})$ acting by automorphisms; so "intrinsic symmetry" of 8 is uninteresting. (The situation is entirely different for curves of higher genus since $g(\mathcal{A}) > 1$ implies $Aut(\mathcal{A})$ is finite.) On the other hand, a *symmetry of an algebraic curve* $\mathcal{A} \subset \mathbb{C}P^2$ will be understood here to be a projective transformation taking $\mathcal{A}$ to itself. One may still use the Riemann surface structure to identify such a symmetry with the automorphism which it induces; but (for a curve of degree $d > 2$) the resulting *group of symmetries* $Sym(\mathcal{A}) \subset Aut(\mathcal{A})$ is typically finite even for $g = 0$ or $g = 1$. For example, a nonsingular cubic curve $\mathcal{A}$ (here, $g(\mathcal{A}) = 1$) has nine inflection points, which must be permuted by any symmetry. As a consequence, it can be shown that $|Sym(\mathcal{A})| = 18$ (see [2], p. 298).

Likewise, the three double points of 8 (which happen to be the inflection points!) are necessarily permuted by any symmetry. The induced Möbius transformation permutes the six t-values $t = \pm e^{i\pi/4}, \pm e^{i3\pi/4}, 0, \infty$ in pairs. Since a Möbius transformation is determined by what it does to three points, it follows that $Sym(8) \subset PGL(2, \mathbb{C})$ has order at most 48. Since the finite subgroups of $PGL(2, \mathbb{C})$ are known to be isomorpic to one of $\mathbb{Z}_n, D_n, A_4, S_4$ or A_5 (see [6], p. 49), very few possibilities remain for $Sym(8)$ as an abstract group.

In fact, the octahedral symmetry group $Sym(8) \simeq \mathcal{O}$ appears at a glance, once we adopt the following *trilinear coordinates* (see, e.g., [5]) associated to the double

points $\mathcal{I}, \mathcal{J}, \mathcal{K}$:

$$\alpha = x + iy, \quad \beta = x - iy, \quad \gamma = cz \tag{6.3}$$

$$x = \frac{\alpha + \beta}{2}, \quad y = \frac{\alpha - \beta}{2i}, \quad z = \frac{\gamma}{c} \tag{6.4}$$

From now on we will make extensive use of α, β, γ, either as new coordinates for $\mathbb{C}^3$ or as homogeneous coordinates in $\mathbb{C}P^2$. Also, we will use the corresponding non-homogeneous coordinates $z = \alpha/\gamma, w = \beta/\gamma$ for $\mathbb{C}^2$; these are known as *isotropic* (or *conjugate*) *coordinates* (where usually $c = 1$).

A particularly symmetric form of the lemniscate equation follows:

$$0 = F(x, y, z) = G(\alpha, \beta, \gamma) = \beta^2\gamma^2 + \alpha^2\gamma^2 + \alpha^2\beta^2 \tag{6.5}$$

Since G is symmetric under all permutations and sign changes of the three variables α, β, γ, it follows that the octahedral group $\mathcal{O}$ acts on the lemniscate. As an overall sign change in homogeneous coordinates has no effect on points $p \in \mathbb{C}P^2$, the above symmetries are represented *one-to-one* by the 24 matrices $\mathbf{M} \in \mathcal{O} \subset SO(3)$. Since $\mathcal{O} \simeq S_4$ does not occur as a subgroup of $\mathbb{Z}_{48}$ or D_{24}, it follows that $Sym(8) \simeq \mathcal{O}$.

For a more concrete mental image, $\mathcal{O}$ may be allowed to act instead on the real linear span of the new basis vectors:

$$\hat{\mathcal{I}} = \frac{1}{2}(1, -i, 0), \quad \hat{\mathcal{J}} = \frac{1}{2}(1, i, 0), \quad \hat{\mathcal{K}} = (0, 0, \frac{1}{c}) \tag{6.6}$$

[**NOTE:** Triples (α, β, γ) will be understood, henceforth, to represent points in $\mathbb{C}^3$ with respect to the *new coordinates*, except where explicitly noted to the contrary; likewise for $[\alpha, \beta, \gamma] \in \mathbb{C}P^2$. Thus, $\hat{\mathcal{I}} = (1, 0, 0), \hat{\mathcal{J}} = (0, 1, 0), \hat{\mathcal{K}} = (0, 0, 1)$. (Our use of pair notation, such as (x, y) or (z, w), will usually be clear from the context.)] Specialization to $\alpha, \beta, \gamma \in \mathbb{R}$ gives our "standard copy" of Euclidean 3-space:

$$L_0 = \{p = (\alpha, \beta, \gamma) = \alpha\hat{\mathcal{I}} + \beta\hat{\mathcal{J}} + \gamma\hat{\mathcal{K}} : \alpha, \beta, \gamma \in \mathbb{R}\} \tag{6.7}$$

The "standard octahedron" in L_0 has vertices $\pm\hat{\mathcal{I}}, \pm\hat{\mathcal{J}}, \pm\hat{\mathcal{K}}$ (not $\pm\hat{\mathbf{i}}, \pm\hat{\mathbf{j}}, \pm\hat{\mathbf{k}}$), and the 24 octahedral symmetries of the lemniscate are easily recognized.

For instance, the symmetry $f(x, y) = f(-x, -y)$ is equivalent to the projective transformation $[\alpha, \beta, \gamma] \mapsto [\alpha, \beta, -\gamma]$, which in turn corresponds to π-rotation about the γ-axis in L_0. This is one of the three *tetrahedral half-turns* in $\mathcal{O}$. Likewise, $f(x, y) = f(-x, y)$ is equivalent to $[\alpha, \beta, \gamma] \mapsto [-\beta, -\alpha, \gamma] = [\beta, \alpha, -\gamma]$, which corresponds to π-rotation about axis $\alpha = \beta, \gamma = 0$. This is one of six *non-tetrahedral half-turns* in $\mathcal{O}$ (which fix no vertex); recall that any one of these and, say, the $2\pi/3$-rotation $(\alpha, \beta, \gamma) \mapsto (\gamma, \alpha, \beta)$ generate $\mathcal{O}$.

So far we have considered only holomorphic (projective) symmetries of 8. But the previous section's discussion of the disdyakis dodecahedron suggests that certain *antiholomorphic* symmetries are what we need for triangulation of 8. We now describe the required antiholomorphic symmetries explicitly. If our explanations compound the confusion of real/complex and projective/vector spaces, the meanings of our constructions will be fleshed out in subsequent sections.

Let R_0 denote the "complex conjugation operator" (real structure) on $\mathbb{C}^3 = \{(\alpha, \beta, \gamma)\}$: $(\alpha, \beta, \gamma) \overset{R_0}{\longmapsto} (\bar{\alpha}, \bar{\beta}, \bar{\gamma})$. Then $-R_0$ also preserves Equation 6.5, and generates with $\mathcal{O}$ the group of holomorphic/antiholomorphic symmetries:

$$\hat{\mathcal{O}} = \mathcal{O} \cup \{-R_0\mathbf{M} : \mathbf{M} \in \mathcal{O}\} \tag{6.8}$$

The reason for the *minus* sign is to give $\hat{\mathcal{O}}$ a remarkable, dual role: $\hat{\mathcal{O}}$ may be viewed either as the full symmetry group of $8 \subset \mathbb{C}P^2$ or as the full symmetry group of the *standard disdyakis dodecahedron* $\mathcal{G}_9 \subset S^2 \subset L_0$. On the one hand, $\hat{\mathcal{O}}$ acts on $\mathbb{C}P^2$, and the "$-$" in the operator $-R_0$ plays no role. On the other hand, $\hat{\mathcal{O}}$ acts on L_0 and R_0 does nothing.

For triangulation, the "mirror symmetries" in $\hat{\mathcal{O}}$ are the essential ones. Observe that $\mathrm{ord}(-R_0\mathbf{M}) = \mathrm{ord}(\mathbf{M})$ if $\mathbf{M} \in \mathcal{O}$ has even order, and $\mathrm{ord}(-R_0\mathbf{M}) = 2\,\mathrm{ord}(\mathbf{M})$ if $\mathbf{M}$ has odd order. It follows that $\hat{\mathcal{O}}$ contains precisely 10 antiholomorphic, involutive symmetries. The order-two elements $\mathbf{M}_2 \in \mathcal{O}$ give the desired 9 mirror symmetries $-R_0\mathbf{M}_2$; while $\mathbf{M}_2$ takes a 2-plane $\mathcal{P} \subset L_0$ to itself by π-rotation, $-R_0\mathbf{M}_2$ fixes the plane pointwise. We list the $9 = 3 + 6$ "outputs" (the fourth of which gives the involution $\mathcal{R}$ discussed in the introduction):

$$(-\bar{\alpha}, \bar{\beta}, \bar{\gamma}),\ (\bar{\alpha}, -\bar{\beta}, \bar{\gamma}),\ (\bar{\alpha}, \bar{\beta}, -\bar{\gamma}) \tag{6.9}$$

$$(\bar{\beta}, \bar{\alpha}, \bar{\gamma}),\ (\bar{\gamma}, \bar{\beta}, \bar{\alpha}),\ (\bar{\alpha}, \bar{\gamma}, \bar{\beta}),\ (-\bar{\beta}, -\bar{\alpha}, \bar{\gamma}),\ (-\bar{\gamma}, \bar{\beta}, -\bar{\alpha}),\ (\bar{\alpha}, -\bar{\gamma}, -\bar{\beta}) \tag{6.10}$$

By setting any of these equal to (α, β, γ), one can read off the corresponding mirror $\mathcal{P}$, whose intersection with $S^2 \subset L_0$ is one of the 9 geodesics of $\mathcal{G}_9$.

Remark 6.1. The *tenth* involution is $-R_0 Id = -R_0$, which is not a "mirror symmetry" (of 8 or $\mathcal{G}_9$). We note that there are two *non-equivalent* real structures on the complex projective line $\mathbb{C}P^1 = \{[z_1, z_2]\}$; that is, up to conjugation by automorphisms, an antiholomorphic involution is given either by complex conjugation $[z_1, z_2] \leftrightarrow [\bar{z}_1, \bar{z}_2]$ or by the *antipodal map* $[z_1, z_2] \leftrightarrow [-\bar{z}_2, \bar{z}_1]$. The latter corresponds to $-R_0$, via stereographic projection, and has empty fixed point set. On the other hand, the fixed point set of an involution of the first type is a simple closed curve in $\mathbb{C}P^1$. In particular, $-R_0\mathbf{M}_2$ fixes the points of a geodesic in $\mathcal{G}_9$, as already noted. Likewise, it will be seen below that $-R_0\mathbf{M}_2$ may be regarded as a Riemannian symmetry of 8 (with respect to the metric referred to in Theorem 1.1) and fixes the points of a geodesic in 8 .

7. Inversion: quadrics and trinodal quartics

Above, $Sym(8)$ appears as a subgroup $\mathcal{O} \subset SO(3, \mathbb{R}) \subset SO(3, \mathbb{C})$. Just as $SO(3, \mathbb{R})$ may be viewed as acting on Euclidean 3-space $L_0 \simeq \mathbb{R}^3$ by (orientation-preserving) linear isometries, the larger group $SO(3, \mathbb{C})$ preserves the complex extension of the Euclidean form—the *fundamental form* on $\mathbb{C}^3 = \{v = (\alpha, \beta, \gamma)\}$:

$$\Phi(v) = v \cdot v = \alpha^2 + \beta^2 + \gamma^2 \tag{7.1}$$

In particular, $SO(3,\mathbb{C})$ preserves the *light cone* $\Phi_0 = \Phi^{-1}(0)$, as do scalar matrices λId, $\lambda \in \mathbb{C}^\times$. Projectivization of the light cone gives the *standard quadric* $Q \subset \mathbb{C}P^2$, which is topologically a sphere, with $Sym(Q) = SO(3,\mathbb{C})$. In x, y, z-coordinates, we recognize Q as a rectangular hyperbola: $2x^2 - 2y^2 + c^2z^2 = 0$.

This brings us almost full circle; for one of our first observations about the lemniscate was that it may be obtained by applying inversion $z \mapsto 1/z$ to a rectangular hyperbola. The relationship $\sigma(\supset\!\subset) = 8$ may now be understood more fully in the setting of projective geometry, where inversion is realized as the basic *quadratic transformation*—which we will also denote by σ. As geometers have long known (see, e.g., [5], Chapter XVII), the trinodal quartics $\mathcal{Q}$ are associated one-to-one with quadrics Q via σ. We will describe the construction as it applies to any real, trinodal quartic $\mathcal{Q}$ with double points placed at $\mathcal{I}, \mathcal{J}, \mathcal{K}$ (as may always be done by projective transformation), then return to the lemniscate.

First consider the *fundamental triangle* $\triangle$ with "vertices" $\mathcal{I}, \mathcal{J}, \mathcal{K}$ and "edges" $\mathcal{I}\mathcal{J}$, $\mathcal{J}\mathcal{K}$, $\mathcal{K}\mathcal{I}$. In associated trilinear coordinates α, β, γ, the equation for $\triangle$ is $\alpha\beta\gamma = 0$. *Inversion* with respect to $\triangle$ is defined by:

$$\sigma[\alpha,\beta,\gamma] = [\frac{1}{\alpha}, \frac{1}{\beta}, \frac{1}{\gamma}] = [\beta\gamma, \alpha\gamma, \alpha\beta] \tag{7.2}$$

The precise relationship between $\sigma[\alpha,\beta,\gamma]$ and $\sigma(z) = 1/z$ will be explained below. For now we observe that σ is well-defined, as a mapping, except at the vertices $\mathcal{I}, \mathcal{J}, \mathcal{K}$. On the complement of the fundamental triangle, $\mathbb{C}P^2 \setminus \triangle$, σ defines an involution. On the other hand, σ collapses each edge of $\triangle$ to its opposite point; specifically, the preimage of $\mathcal{K}$ is the ideal line $\gamma = 0$. We mention that σ plays an important role among *birational transformations* of $\mathbb{C}P^2$. Though the *Cremona group* consisting of birational transformations of $\mathbb{C}P^n$ is not well understood in general, it is known that for $n = 2$, the full group is generated by σ and projective transformations. As a consequence, σ is essential to the classical theory of singularities of algebraic curves.

Now it is easy to see why $Q = \sigma\mathcal{Q}$ has degree two. The two points at K of the trinodal quartic $\mathcal{Q} = \sigma Q$ are the σ-images of a pair of points $c_\pm = Q \cap \mathcal{I}\mathcal{J}$; i.e., Q has two ideal points and must be a quadric. (Likewise, the double points of $\mathcal{Q}$ at $\mathcal{I}$ and $\mathcal{J}$ are the respective σ-images of pairs $a_\pm = Q \cap \mathcal{J}\mathcal{K}, b_\pm = Q \cap \mathcal{K}\mathcal{I}$; it follows that the quartics $\mathcal{Q}$ with double points at $\mathcal{I}, \mathcal{J}, \mathcal{K}$ determine and are determined by the six points of intersection $Q \cap \triangle = \{a_\pm, b_\pm, c_\pm\}$.) Turning things around, we may produce a trinodal quartic by inversion of a quadric (if it is irreducible and does not contain $\mathcal{I}, \mathcal{J}$, or $\mathcal{K}$). In particular, inversion of the standard quadric Q gives the lemniscate equation $0 = \sigma^*\Phi = (\beta\gamma)^2 + (\alpha\gamma)^2 + (\alpha\beta)^2$.

Regarding the lemniscate as $8 = \sigma(Q)$ gives insight into its octahedral symmetry. If M is a projective transformation, then $\sigma^{-1}M\sigma$ is defined and analytic almost everywhere; M extends to a projective transformation precisely when M preserves the fundamental triangle $\triangle$. (If M does not preserve $\triangle$, then $\sigma^{-1}M\sigma = \sigma M\sigma$ fails

to be one-to-one; conversely, any $M \in Sym(\triangle) \subset GL(3,\mathbb{C})$ may be factored as a product PD of permutation and diagonal matrices, and $\sigma PD\sigma = P\sigma D\sigma = PD^{-1}$.)

In particular, $M \in Sym(8) \subset Sym(\triangle)$ defines a symmetry $M = \sigma^{-1}M\sigma$ of Q, as we already knew: $Sym(8) \subset SO(3,\mathbb{R}) \subset SO(3,\mathbb{C}) = Sym(Q)$. On the other hand, suppose M is a symmetry of Q and also preserves $\triangle$. Then $M = \sigma M\sigma^{-1}$ defines a symmetry of 8 (note that a diagonal matrix $D \in SO(3,\mathbb{C})$ satisfies $D = D^{-1}$). Thus, the explanation of octahedral symmetry of 8 may be summarized:

$$Sym(8) = SO(3,\mathbb{C}) \cap Sym(\triangle) = \mathcal{O} \tag{7.3}$$

To include orientation-reversing symmetries, we need only make the further observation that σ commutes with the generating antiholomorphic operator $-R_0$ (see Equation 6.8). Then we recover the full symmetry group of 8 as:

$$FullSym(8) = \hat{SO}(3,\mathbb{C}) \cap \hat{Sym}(\triangle) = \hat{\mathcal{O}} \tag{7.4}$$

As above, the *hat* denotes the group generated by $-R_0$, together with the original group. In particular, note that $\hat{\mathcal{O}}$ belongs to $\hat{SO}(3,\mathbb{C})$—not $O(3,\mathbb{C})$—though it is isomorphic to a subgroup of the latter.

In the classical theory of algebraic curves, *trilinear coordinates* and *quadratic transformation* are two important constructions based on a fundamental triangle $\triangle$. Choosing the vertices of $\triangle$ to coincide with the nodes $\mathcal{I}, \mathcal{J}, \mathcal{K}$ of the lemniscate, one may hardly be surprised that the resulting coordinates α, β, γ and quadratic transformation σ shed light on the lemniscate's geometry.

It is helpful to have a mental picture relating these constructions to our earlier discussion of the lemniscate. We recall that an *isotropic line* in $\mathbb{C}P^2$ is a complex line passing though one of the circular points $\mathcal{I}, \mathcal{J}$. A line through $\mathcal{J}$, e.g., has equation of the form $\alpha - \alpha_0\gamma = 0$ and intersects the ("traditional") real plane $\mathbb{R}^2 = \{[x,y,1] : x,y \in \mathbb{R}\} = \{[\alpha,\bar{\alpha},1] : \alpha \in \mathbb{C}\}$ at $[\alpha_0,\bar{\alpha}_0,1]$. Let $\mathcal{A}$ be a real algebraic curve $0 = F(x,y,z)$ (F has real coefficients with respect to the *original coordinates* x,y,z). *Isotropic projection from* $\mathcal{J}$ assigns to $P \in \mathcal{A}$ the corresponding intersection point of its isotropic line $\overline{\mathcal{J}P}$ with the real plane ($\pi_{\mathcal{I}}$ is defined similarly):

$$\pi_{\mathcal{J}}(P) = \overline{\mathcal{J}P} \cap \mathbb{R}^3 \tag{7.5}$$

Note that a real point $P \in \mathcal{A}_{\mathbb{R}} = \mathcal{A} \cap \mathbb{R}^3$ projects to itself, $\pi_{\mathcal{J}}(P) = P$. This is important for visualization of $\mathcal{A}$, since it allows the complex points of $\mathcal{A}$ to be viewed in planar projection, filling in the "missing points" around $\mathcal{A}_{\mathbb{R}}$. Interesting features of $\mathcal{A}$ are thus displayed; for example, the (real) foci of $\mathcal{A}$ stand out as ramification points of $\pi_{\mathcal{J}}$ (since they correspond to isotropic tangent lines to $\mathcal{A}$).

Further, it now emerges that complex notation $z = x+iy$—utilized almost from the beginning of our study of the lemniscate—was no mere convenience. Viewing z as one of *two* isotropic coordinates $z = x + iy, w = x - iy$ on $\mathbb{C}^2 = \{(z,w)\}$, the redundant representation of planar points $(z,\bar{z}) \in \mathbb{R}^2$ enables us to leave the real plane simply by replacing $z,\bar{z}$ with independent variables z,w. Thus, for instance,

if $f(z)$ is analytic on some domain $D \subset \mathbb{C} \simeq \mathbb{R}^2$, then f extends to an analytic mapping of two complex variables by the formula:

$$F(z,w) = (f(z), \overline{f(\bar{w})}) \tag{7.6}$$

In particular, $f(z) = 1/z$ extends to $F(z,w) = (1/z, 1/w)$. With $z = \alpha/\gamma, w = \beta/\gamma$, the homogeneous coordinate expression for inversion follows, and the new meaning of σ is seen to be an extension of the old.

Remark 7.1. We are now in a position to straighten out a curious turn in our graphical exploration of the lemniscate. Recall that the mapping $j_-(\pi(z))$ takes a certain pair of circles in $\mathcal{G}_6$ to 8 and $\asymp$; the circles are related by $2\pi/3$-rotation of S^2, while 8 and $\asymp$ are interchanged by $\sigma(z) = 1/z$.

Here's how the imposter σ mimics a symmetry in $\mathcal{O}$. First note that the order-three symmetry $[\alpha, \beta, \gamma] \mapsto [\gamma, \alpha, \beta]$ may be re-expressed in non-homogeneous coordinates as $(\alpha, \beta) \overset{m_3}{\mapsto} (1/\beta, \alpha/\beta)$, while inversion is given by $(\alpha, \beta) \overset{\sigma}{\mapsto} (1/\alpha, 1/\beta)$. Now if (α, β) parameterize s the original real curve 8, then so does (β, α) (because of the real symmetry $(x, y) \leftrightarrow (x, -y)$), and so $\sigma(8) = \asymp$ has parameterization $(1/\beta, 1/\alpha)$. Viewed in isotropic projection, the latter cannot be distinguished from $(1/\beta, \alpha/\beta)$, both being represented by $1/\beta$ as curves in the complex plane.

8. Triangulation of the lemniscate

In this section we describe the triangulation $\mathcal{T}$ of the lemniscate. First we sketch how the lemniscate's nine mirrors of reflection symmetry may be used to determine $\mathcal{T}$ abstractly. Then we use a simple, equivariant parameterization of the lemniscate to describe 8, more concretely, as the topological image of the disdyakis dodecahedron $\mathcal{G}_9 \approx S^2$ (triangulated sphere). In order to present the main ideas without further delay we defer much of the relevant background to Appendix A (for mirrors) and Appendix B (for equivariant parameterization).

The 9 mirrors of 8 distinguish the face points, edge points, and vertices of $\mathcal{T}$ as follows. A point p lies on $0, 1, 2, 3$ or 4 mirrors and is stabilized by a subgroup $\hat{\mathcal{O}}_p$ of order $1, 2, 4, 6$ or 16. (The groups $\hat{\mathcal{O}}_p$ are generated by the incident mirrors, except in the last case, where there is also a mirror swapping the two copies of a double point.) In particular, face points have $\hat{\mathcal{O}}$-orbit lengths $|p| = 48$, edge points are characterized by $|p| = 24$, and $|p| = 3, 8$ and 12 for the three types of vertices. (Note that these lengths agree with Equation 5.1, except that the six octahedral vertices, which are double points, now have orbit length 3 instead of 6.)

To describe the faces of 8, it suffices to describe their interiors. Namely, any face point p lies in a *face interior* $\mathrm{int}(\mathcal{F}_p)$, the union of all connected open subsets of 8 containing p whose points q all have orbit length $|q| = 48$. Recall from Section 6 that each mirror divides $8 \simeq \mathbb{C}P^1$ into two "halves". Thus,

int($\mathcal{F}_p$) may be described, alternatively, as the set of all face points q lying on the same "side" of each mirror as p. The face $\mathcal{F}_p$, defined as the closure of int($\mathcal{F}_p$), is bounded by edges $\mathcal{E}_{p_j} = \mathcal{F}_p \cap \mathcal{M}_j$, one for each mirror $\mathcal{F}_p$ intersects. The vertices of $\mathcal{F}_p$ are the pairwise intersections of edges $\mathcal{E}_{p_j} \cap \mathcal{E}_{p_k}$. Since $\hat{\mathcal{O}}$ permutes the 9 mirrors of 8 it also permutes the faces, edges and vertices just described; $\mathcal{T}$ is $\hat{\mathcal{O}}$-*invariant* in the sense that $\hat{\mathcal{O}}$ acts by simplicial maps.

We have not yet fully described $\mathcal{T}$; e.g., we have not shown that the faces $\mathcal{F}_p$ are "triangular". There is in fact enough data to determine a simplicial map from $\mathcal{G}_9$ to $\mathcal{T}$, owing to the fact that the mirrors of $\mathcal{G}_9$ and 8 come from the same involutions $-R_0\mathbf{M}_2$, listed in Equations 6.9, 6.10. However, a more concrete explanation of the equivalence $\mathcal{G}_9 \simeq \mathcal{T}$ follows directly from a simple parameterization of the lemniscate which we now describe.

We start with the *standard parameterization of the quadric* Q, the embedding $\psi : \mathbb{C}P^1 \to \mathbb{C}P^2$ given by the formula:

$$[\mu, \nu] \overset{\psi}{\longmapsto} [\alpha, \beta, \gamma] = [\mu^2 - \nu^2, i(\mu^2 + \nu^2), -2\mu\nu] \tag{8.1}$$

Alternatively, the sphere $a^2 + b^2 + c^2 = 1$ may be taken as domain in place of $\mathbb{C}P^1$. That is, a point $r = (a, b, c) \in S^2$ corresponds, via stereographic projection (from the *south pole*), to $[\mu, \nu] = [1 + c, a + ib] \in \mathbb{C}P^1$; so we may regard the standard parameterization instead as a map $\varphi : S^2 \to \mathbb{C}P^2$, namely, $\varphi(a, b, c) = \psi(1 + c, a + ib)$.

Equation 8.1 satisfies $\alpha^2 + \beta^2 + \gamma^2 = 0$ and, in fact, ψ and φ parameterize the quadric. These maps are also suitably *equivariant*—a property we now describe in the case of φ. As observed in Section 6, rotation matrices $\mathbf{M} \in SO(3)$ may be allowed to act on $L_0 \simeq \mathbb{R}^3$ and also, as projective transformations, on $\mathbb{C}P^2$. Then φ and $\mathbf{M}$ commute: $\varphi \circ \mathbf{M} = \mathbf{M} \circ \varphi$. The corresponding property for ψ is equivariance with respect to the adjoint map $\mathrm{Ad} : SU(2) \to SO(3)$. A fuller account of these results is developed in Appendix B.

Note that the equivariance properties of ψ and φ extend to orientation-reversing symmetries. Here it suffices to consider a single instance; namely, if $\psi(\mu, \nu) = [\alpha, \beta, \gamma]$, then $\psi(\bar{\mu}, \bar{\nu}) = [\bar{\alpha}, -\bar{\beta}, \bar{\gamma}]$, so ψ intertwines the canonical antiholomorphic involution in $\mathbb{C}P^1$ with the second of the "octahedral reflections" of $\mathbb{C}P^2$ given by Equation 6.9. As for φ, note that complex conjugation of $[\mu, \nu] = [1 + c, a + ib]$ corresponds to reflection of $\mathbb{R}^3$ in the α, γ-*plane*. Since the latter corresponds to the same element of $\hat{SO}(3, \mathbb{R})$ as the above octahedral reflection of $\mathbb{C}P^2$, we may summarize the situation in the simplest terms:

Proposition 8.1. *The standard parameterization of* Q *is* $\hat{SO}(3, \mathbb{R})$*-equivariant, i.e.,* $\varphi \circ \mathbf{T} = \mathbf{T} \circ \varphi$*, for each* $\mathbf{T} \in \hat{SO}(3, \mathbb{R})$.

The natural parameterization of the lemniscate, $\sigma\circ\varphi : \mathcal{G}_9 \to 8$, is likewise equivariant—but with respect to the smaller group $\hat{\mathcal{O}}$. This follows from the fact, already observed, that the inversion σ commutes with elements of $\hat{\mathcal{O}}$. As a consequence of equivariance, $\sigma\circ\varphi : \mathcal{G}_9 \to 8$ is necessarily a simplicial map; here we note that $\sigma\circ\varphi$ is $1-1$ except on octahedral vertices, and maps faces of $\mathcal{G}_9$ homeomorphically onto faces of $\mathcal{T}$. Intrinsically, the triangulated lemniscate is indeed a copy of $\mathcal{G}_9$, with octahedral symmetry now realized as a subgroup of the projective group.

The previous paragraph completes our description of the symmetrical embedding and $\hat{\mathcal{O}}$-invariant triangulation of $8\subset \mathbb{C}P^2$ as a disdyakis dodecahedron (modulo the discussion of equivariance in Appendix B). This is the main content of Theorem 1.2, lacking only the translation into Riemannian language, the discussion of geodesics, critical points of Gaussian curvature, etc. (the subject of the next section).

Along the way, we have touched on a variety of topics in our exploration of "hidden" structure of 8. Let us now work our way back to the description of 8 in simplest terms and take a fresh look at our earliest graphical observations. We begin by expressing ψ and φ in non-homogeneous coordinates. That is, we write $(z,w)=\varphi(r)=\psi(\zeta)$, with $r=(a,b,c)\in S^2$, $\zeta=\frac{\mu}{\nu}=\frac{1+c}{a+ib}\in\mathbb{C}P^1$, and $(z,w)=(\alpha/\gamma,\beta/\gamma)\in\mathbb{C}P^2$. Comparing Equations 8.1, 2.3, brings us back to the Joukowski maps, $z=-j_-(\zeta),\ w=-ij_+(\zeta)$—whose special role we are finally in a position to understand.

All that remains is to apply inversion to parameterize 8:

$$(z,w)=\sigma\circ\psi(\zeta)=\left(\frac{-1}{j_-(\zeta)},\frac{-1}{ij_+(\zeta)}\right)=\left(\frac{2\zeta}{1-\zeta^2},\frac{2i\zeta}{1+\zeta^2}\right) \tag{8.2}$$

Points on 8 are viewed in $\mathbb{C}\simeq\mathbb{R}^2$ via isotropic projection $\pi_{\mathcal{J}}$, that is, using the first coordinate function $z(\zeta)=\frac{2\zeta}{1-\zeta^2}$. In this sense, the real lemniscate $8_{\mathbb{R}}$ turns out to be the z-image of the line $\zeta(t)=(1-i)t,\ t\in\mathbb{R}$—one of the nine "circles" of $\pi(\mathcal{G}_9)$. The image of the full disdyakis dodecahedron $z(\pi(\mathcal{G}_9))$ is identical to $j_-(\pi(\mathcal{G}_9))$ (because of the symmetry $z(\pi(\mathcal{G}_9))=-1/z(\pi(\mathcal{G}_9))$), and is a familiar-looking figure.

Specifically, applying $z(\zeta)$ to Figure 7 b) (or $z(\frac{1+c}{a+ib})$ to Figure 7 a)) results in two identical sheets, each of which resembles Figure 8. We may understand the branched double covering $z=\pi_{\mathcal{J}}\circ\sigma\circ\psi : \mathbb{C}P^1\to\mathbb{C}P^1$ as follows. Since 8 is a bicircular quartic, most isotropic lines through the circular point $\mathcal{J}$ also meet 8 in two finite points. The exceptions are the two tangent lines to 8 at $\mathcal{J}$ which mark the pair of foci $\pm i$; these are the ramification points of z. The interior of the unit circle $|\zeta|<1$ is mapped by $z(\zeta)$ (the upper hemisphere is mapped by $z(\frac{1+c}{a+ib})$) onto the slit domain obtained by removing the vertical

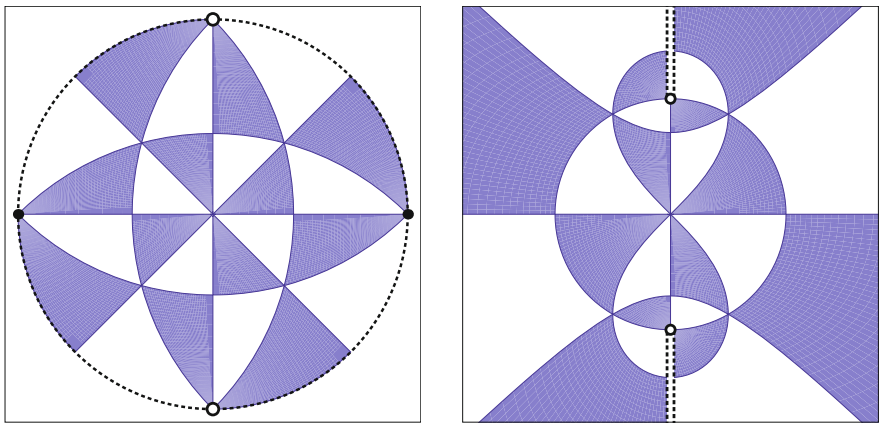

FIGURE 8. Interior of disk (left) maps by $z(\zeta) = \frac{2\zeta}{1-\zeta^2}$ to one of two identical sheets (right) of $\pi_{\mathcal{J}}(8)$.

rays $z = iy,\ |y| \geq 1$; likewise for the exterior of the unit circle. Noting also that $z(\pm 1) = \infty$ makes Figure 8 easier to understand. Because of the symmetry $z(\zeta) = z(-1/\zeta)$, the interior and exterior of the circle yield two identical sheets, each containing half of the 48 triangles of the lemniscate. Finally, note that only *half* of the real lemniscate $8_{\mathbb{R}}$ lies on each sheet, though the familiar curve seems complete in the figure. Keep in mind that the two lines $\zeta(t) = (1 \pm i)t$ are the preimages of two distinct curves in 8—the real lemniscate $8_{\mathbb{R}}$ and the imaginary lemniscate $8_{i\mathbb{R}} = i8_{\mathbb{R}}$!

9. The Riemannian lemniscate

Theorems 1.1, 1.2 refer to the Riemannian metric on the lemniscate induced by the Fubini-Study metric g on $\mathbb{C}P^2$. For our purposes, the most important property of g is that it is invariant under the action induced by the group $\hat{U}(3)$ of unitary/anti-unitary transformations on $\mathbb{C}^3$; the unitary group $U(3)$ preserves the Hermitian scalar product $\langle\ ,\ \rangle$, and $\hat{U}(3)$ is generated by $U(3)$ together with the operation of complex conjugation of coordinates. For more background on $\hat{U}(3)$, $\langle\ ,\ \rangle$, etc., see Appendix A. For the moment, we note that by our definition of $\langle\ ,\ \rangle$, the basis $\hat{\mathcal{I}},\ \hat{\mathcal{J}},\ \hat{\mathcal{K}}$ is orthonormal (not necessarily so for the original basis $\hat{\mathbf{i}},\ \hat{\mathbf{j}},\ \hat{\mathbf{k}}$).

One way to describe the geometry of $\mathbb{C}P^2$ uses the Hopf projection on the five-sphere $\pi : S^5 \to \mathbb{C}P^2$ (which plays a role also in Appendix B). A point $p \in \mathbb{C}P^2$ (complex line $L \subset \mathbb{C}^3$) corresponds to a great circle $\pi^{-1}(p) \subset S^5$ ($L \cap S^5$). Then the distance between two points $p, q \in \mathbb{C}P^2$ may be defined to be the distance between circles $\pi^{-1}(p)$ and $\pi^{-1}(q)$ in S^5. The required invariance property then follows from the fact that $\hat{U}(3)$ acts isometrically on S^5.

However, we will require explicit formulas describing the geometry of $(\mathbb{C}P^2, g)$ on the infinitesimal level. In order to define the length $\sqrt{g(v,v)}$ of a tangent vector $v \in \mathbb{C}P^2$, we work with homogeneous coordinates. That is, we let $P = (\alpha, \beta, \gamma) \in \mathbb{C}^3$ represent $p = \pi(P) = [\alpha, \beta, \gamma] \in \mathbb{C}P^2$. If now $P(t)$ is a curve passing through $P = P(0)$ with velocity vector $V = P'(0)$, then $p(t) = \pi(P(t))$ is a curve passing through $p = p(0)$ with velocity vector $v = \pi_* V = (\pi \circ P)'(0) \in T_p \mathbb{C}P^2$. If likewise $w = \pi_* W \in T_p \mathbb{C}P^2$, then the Hermitian scalar product of v and w may be defined by the formula:

$$\langle v, w \rangle_p = 2 \frac{\langle V, W \rangle \langle P, P \rangle - \langle V, P \rangle \langle P, W \rangle}{\langle P, P \rangle^2} \tag{9.1}$$

The Fubini-Study metric is the real part $g_p(v,w) = Re[\langle v, w \rangle_p]$. Again, since $\hat{U}(3)$ acts by Euclidean isometries of $\mathbb{C}^3$, it follows that g defines a $\hat{U}(3)$-invariant Riemannian metric on $\mathbb{C}P^2$.

Now consider an algebraic curve $\mathcal{C} \subset \mathbb{C}P^2$. Lengths of (and angles between) tangent vectors to $\mathcal{C}$ may be measured using $g(\ ,\ )$—this is the induced Riemannian structure on $\mathcal{C}$. Further, a convenient formula due to Linda Ness (see [11]) expresses the Gaussian curvature of $(\mathcal{C}, g)$ in terms of partial derivatives with respect to homogeneous coordinates. That is, if a curve $\mathcal{C}$ of degree $d > 1$ is defined by homogeneous polynomial $G(\alpha, \beta, \gamma)$, the curvature at a nonsingular point $p = \pi(P)$ is given in terms of the norms of P and the gradient of G at P and the Hessian determinant of second order partial derivatives of G at P:

$$K(p) = 2 - \frac{\|P\|^6 \, |\text{Hessian}(G)|^2}{(d-1)^6 \, \|\text{grad}(G)\|^6} \tag{9.2}$$

For example, the quadric Q has equation $G(P) = \alpha^2 + \beta^2 + \gamma^2 = 0$, and we obtain $\text{grad}(G) = 2P$, $|\text{Hessian}(G)| = 8$, and $K(p) = 2 - \frac{\|P\|^6 \ 8^2}{\|2P\|^6} = 1$. The standard quadric is indeed the standard unit sphere!

Having warmed up on Q, let us now return to the lemniscate $8 = \sigma(Q)$. Our first conclusion depends only on the invariance property of g.

Proposition 9.1. *Let the lemniscate $\alpha^2\beta^2 + \beta^2\gamma^2 + \gamma^2\alpha^2 = 0$ be regarded as a Riemannian manifold with metric g induced by the Fubini-Study metric on $\mathbb{C}P^2$. Then there are exactly 9 simple closed geodesics in the lemniscate which are fixed-point sets of an isometry.*

Proof. We have already identified the subgroup of the unitary/antiunitary transformations $\hat{\mathcal{O}} \subset \hat{SO}(3, \mathbb{R}) \subset \hat{U}(3)$ preserving the lemnsicate (Equation 6.8), and within this subgroup we have identified the 9 reflection symmetries (Equations 6.9, 6.10). We can now say these reflections are (orientation-reversing) isometries of 8.

The fixed-point set of any such reflection $-R_0\mathbf{M}_2$ is a simple closed curve in $8 \simeq \mathbb{C}P^1$ (though it has one or two self-intersections in $\mathbb{C}P^2$). Such a curve must be a geodesic, since there is a unique shortest geodesic joining any sufficiently nearby points p, q on the curve: A competing path joining p, q has a mirror image of the same length. Besides the nine geodesics already found, no other geodesic could be the fixed point set of an isometry since we have already accounted for all nine antiholomorphic involutions in $\hat{O}$ which have fixed points. □

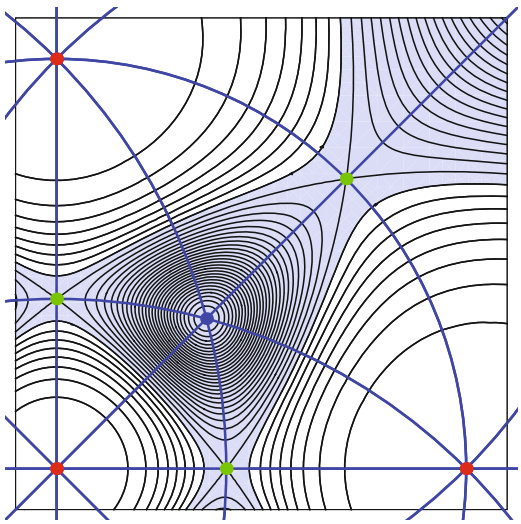

FIGURE 9. Contours and sign of K (region $K < 0$ shaded).

To proceed further, we again make use of the $\hat{\mathcal{O}}$-equivariant parameterization of the lemniscate $\sigma \circ \psi$. In the proposition below, we use this parameterization to pull back the metric and curvature to $\mathbb{C}$; we thus compute lengths of the 9 geodesics, the curvature at all vertices of the triangulation and, above all, are able to produce the appropriately symmetrical contour plot for K, as shown in Figure 1. The level set diagram within a given geodesic triangle must be reproduced throughout the triangulation by iterated reflection in the 9 (light gray) circles/lines of the figure. The structure of level sets is shown in greater detail in Figure 9, which shows a bit more than six complete tiles. Note for instance that the level sets $K = \textit{constant}$, except for the critical level set $K = -1/4$, must meet geodesics orthogonally.

Figure 9 also shows regions of negative curvature (shaded) and positive curvature (unshaded). For this purpose, we have taken advantage of the remarkable circumstance that the significant K-values are so simply related: By choosing a uniform increment $\Delta K = 1/4$, our contour plot is able to accurately

show not only the demarcation curves $K = 0$, but also all three critical level sets $K = -1/4, K = 2, K = -7$ (the latter two consisting of finitely many points). Also striking are the rather large *spherical caps* around $0, 1, i$ (and $-1, -i, \infty$), where K lies in the narrow range $7/4 \leq K \leq 2$. The fact that each of the 9 geodesics cuts through at least two of these already hints at the existence of shorter closed geodesics.

Meanwhile, the negatively curved portion of the lemniscate is connected, and one is tempted to picture it as a "soap film" (minimal surface) spanning six symmetrically arranged wire hoops. But one should not suppose the entire lemniscate is isometrically and $\mathcal{O}$-symmetrically embedded in $\mathbb{R}^3$—this is impossible! The contradiction arises when one considers the lines of principal curvature, say, at one of the minima $K = -7$, and the fact that such a point has non-trivial isotropy.

Proposition 9.2. *Let K be the Gaussian curvature of the lemniscate, and let a, b, c denote the three types of vertices of the triangulation; specifically, a geodesic triangle has angles $\pi/4$ at a, $\pi/3$ at b, and $\pi/2$ at c.*

a) *K has critical points at the $26 = 6+12+8$ disdyakis-dodecahedral vertices with respective K-values:*

$$K_{max} = K(a) = 2, \quad K_{min} = K(b) = -7, \quad K_{saddle} = K(c) = -1/4$$

b) *The opposite sides A, B, C of a geodesic triangle have lengths:*

$$|A| \approx .69, \quad |B| \approx 1.27, \quad |C| \approx 1.40$$

c) *The three geodesics of type B^8 have length $L_1 = 8|B| \approx 10.16$, and the six geodesics $(CA)^4$ have length $L_0 = 4(|A| + |C|) \approx 8.41$. The four piecewise geodesics A^{12}, which zig-zag through the $K < 0$ region and divide the lemniscate into two congruent (but not reflection-symmetric) halves, have length $L_{-1} = 12|A| \approx 8.38 < 8.41$!*

Proof. Since a vertex v has nontrivial stabilizer in $\mathcal{O}$, the point v is automatically critical for the $\mathcal{O}$-invariant function K. Equation 9.2 shows that $K \leq 2$, with equality only at inflection points. Even though the inflection points of the lemniscate (e.g., $a = [0, 0, 1]$) are singular, the curvature is well-behaved on each branch of such a node, with limiting value $K = 2$.

We pull back K to $\mathbb{C}$ using our equivariant parameterization of the lemniscate, $\gamma(u) = \sigma(\psi(u)) = [2(u + u^3), 2i(u - u^3), 1 - u^4]$. In terms of u and its complex conjugate $v = \bar{u}$, we compute the pulled-back function $k = K(\gamma(u))$:

$$k = \ 2 - \frac{9uv(1-u^4)(1-v^4)(1+8uv+8u^3v^3-v^4-u^4+u^4v^4)^3}{2(1+3u^4+3v^4+32u^3v^3+9u^4v^4+u^2v^2(3+v^4)(3+u^4))^3} \qquad (9.3)$$

We note $\gamma(0) = a = [0, 0, 1]$, so the above claim $K(a) = k(0, 0) = 2$ is obvious. Likewise, letting $\omega_8 = \frac{1+i}{\sqrt{2}}$ and $r = \frac{1+\sqrt{3}}{\sqrt{2}}$, we may write $\gamma(\omega_8) = c$ and $\gamma(\omega_8 r) = b$. We thus obtain the following remarkable critical values:

$$K(b) = k(r\omega_8, r\omega_8^{-1}) = 2 - \frac{15925248(70226 + 40545\sqrt{3})}{1769472(70226 + 40545\sqrt{3})} = -7$$

$$K(c) = k(\omega_8, \omega_8^{-1}) = 2 - \frac{147456000(3880899 + 2744210\sqrt{2})}{65536000(3880899 + 2744210\sqrt{2})} = -\frac{1}{4}$$

The gradient $X = \text{grad}K$ has indices $ind_X(a) = ind_X(b) = 1$ and $ind_X(c) = -1$, consistent with the above data and evident in Figure 9.

Finally, the edge lengths $|A|, |B|, |C|$ are computed by substituting convenient parameterization s into Equation 9.1. For example, using $u = t$,

$$|B| = \frac{1}{2}\int_0^1 \sqrt{g(\gamma', \gamma')}dt = \frac{1}{2}\int_0^1 4\frac{\sqrt{1 + 15t^4 + 32t^6 + 15t^8 + t^{12}}}{1 + 8t^2 - 2t^4 + 8t^6 + t^8}dt \approx 1.270$$

Similarly, $\gamma(\omega_8 t)$ has speed $v(t) = 4\frac{\sqrt{1 + 3t^4 + 32t^6 + 3t^8 + t^{12}}}{1 + 8t^2 + 2t^4 + 8t^6 + t^8}$, and gives

$$|C| = \int_0^{1/r} v(t)dt \approx 1.404, , \quad |A| = \int_{1/r}^1 v(t)dt \approx 0.698 \qquad \square$$

Remark 9.3. It is known that any Riemannian 2-sphere has at least three simple closed geodesics, for topological reasons. In the case of the lemniscate, symmetry enabled us to locate nine. The previous proposition suggests that there might exist four more simple geodesics. Namely, the piecewise geodesics of type A^{12} lie in the "soap film" region of negative curvature. One can imagine deforming A^{12}, say, by the negative gradient of energy $\mathcal{E}(\gamma) = \int_0^1 g(\gamma', \gamma'))dt$, defined on an appropriate space of loops in the lemniscate. One would not be surprised that such a deformation would converge to a locally minimizing, simple geodesic—see Figure 10 a). In the following proposition we use instead another symmetry argument, which very likely produces the same four geodesics.

Proposition 9.4. *In addition to the* 9 *geodesics of reflection symmetry, there are* 4 *simple closed geodesics in the lemniscate. Each of these is fixed by a subgroup of* $\hat{\mathcal{O}}$ *of order* 12*, and is shorter than any of the* 9 *geodesics. Numerical computation shows that the* 4 *geodesics are locally length minimizing, with length* $L \approx 7.65$*.*

Proof. Consider one of the geodesic triangles $\triangle abc$, with right angle at c and "hypotenuse" C which is part of a geodesic $\Gamma = (CA)^4$. Along Γ, the point p

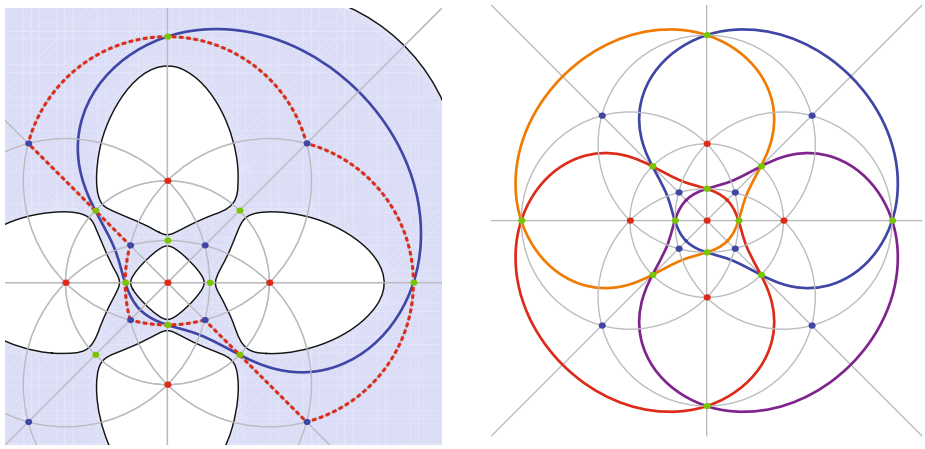

FIGURE 10. a) Piecewise geodesic (dashed) shortens to smooth geodesic (solid). b) Thirteen simple closed geodesics in the Riemannian Lemniscate.

closest to c is connected to c by a simple geodesic γ_1 of length l_1. This geodesic meets Γ perpendicularly (one of the local principles we invoke, for which Euclidean reasoning is valid), so γ_1 may be reflected "across the hypotenuse" to a new geodesic $R_C\gamma_1$. Then the union $\gamma_2 = \gamma_1 \cup R_C\gamma_1$ is a smooth geodesic of length $2l_0$. Next, since c is one of the two fixed points of a π-rotation $r_c \in \mathcal{O}$, we may again double γ_2 and form a smooth geodesic $\gamma_4 = \gamma_2 \cup r_c\gamma_2$ of length $4l_0$. The last operation can be iterated, using the new endpoint as fixed point of a π-rotation. The procedure produces a closed geodesic γ of length $12l_0$; in fact, γ may be described as the orbit of γ_1 under the order 12 subgroup of $\hat{\mathcal{O}}$ generated by R_C and r_c. This subgroup is best understood as the group generated by R_C and a dihedral subgroup $D_3 \subset \hat{\mathcal{O}}$. Namely, $D_3 = \langle F, T : F^2 = T^3 = FTFT = 1\rangle$ is generated by $F = R_C r_c R_C$ and $T = R_C r_c R_C r_c$.

By construction, γ is shorter than the piecewise geodesics A^{12} of the previous proposition, hence, shorter than the nine geodesics $(CA)^4$ and B^8. It remains to show that γ is simple. We already know γ_1 is simple; the question is whether the 12 images of γ_1 might intersect each other. Intuitively, γ_1 ought to lie within its triangle $\triangle abc$, and the conclusion should follow.

A simple argument shows that this is in fact the case. Suppose, to the contrary, that γ_1 does not lie in $\triangle abc$. Then γ_1 can be replaced by a piecewise-smooth "billiard path" $\tilde{\gamma}_1 \subset \triangle abc$ of the same length. One may think of the rule: *Angle of incidence equals angle of reflection.* Put another way, since $\hat{\mathcal{O}}$ acts simply transitively on the 48 triangles, each leg of γ_1 passing through another triangle is mapped by a unique element of $\hat{\mathcal{O}}$ to its congruent image

in $\triangle abc$, and the resulting collection of images $\tilde{\gamma}_1$ is easily seen to form a piecewise-smooth path of the same length. But in fact, $\tilde{\gamma}_1$ cannot "bounce" even once, since a shortest path between two points cannot have "corners"; a local detour which cuts off a corner decreases length. Nor can $\tilde{\gamma}_1$ meet A or B tangentially, by uniqueness for geodesics. Except for its endpoints, γ_1 actually lies entirely in the interior of $\triangle abc$.

Finally, the ODE system for geodesics may be solved with high precision, and the expected periodic solutions may be numerically found by a shooting method. The resulting graphical output is shown in Figure 10. In Figure 10 a), one such geodesic is shown, together with a plot of the region $K < 0$. Since the geodesic clearly lies inside the region $K < 0$, it follows by a standard result of Riemannian geometry that this geodesic is shorter than nearby closed curves. □

Appendix A. Reflections in $\mathbb{R}^3$, $\mathbb{C}^3$ and $\mathbb{C}P^2$

In this section we discuss first *Lagrangian subspaces* $L \subset \mathbb{C}^3$; these *mirrors* are copies of $\mathbb{R}^3$ and are fixed-point sets of antiholomorphic involutions (*real structures*) $R_L : \mathbb{C}^3 \to \mathbb{C}^3$. The latter take complex lines to complex lines, and define *Lagrangian reflections* of $\mathbb{C}P^2$. Using the original coordinates, one of these mirrors is given by $L_1 = \{p \in \mathbb{C}^3 : x, y, z \in \mathbb{R}\}$, corresponding to the usual real structure $R_{L_1}(x, y, z) = (\bar{x}, \bar{y}, \bar{z})$ on $\mathbb{C}^3$. For any real algebraic curve $F(x, y, z) = 0$ (F has real coefficients), $R_1 = R_{L_1}$ induces an antiholomorphic symmetry.

Mirrors and their reflections will be expressed in terms of the "base" Lagrangian subspace L_0. We subsequently restrict our attention to certain Lagrangian subspaces L which, like L_1, have 2-dimensional *real part*, $\mathcal{P} = L \cap L_0$. In fact, each linear 2-plane in Euclidean 3-space $\mathbb{R}^3 = L_0$ is the real part of such a Lagrangian subspace $L = L_{\mathcal{P}}$. In particular, the reflection symmetries of the disdyakis dodecahedron will be seen to extend to the Lagrangian reflection symmetries of 8 required for triangulation.

Considering the role of L_0, we let $\alpha, \beta, \gamma \in \mathbb{C}$ serve as "standard coordinates" for $\mathbb{C}^3 = \{v = (\alpha, \beta, \gamma)\} = L_0 \oplus JL_0$. The decomposition of $\mathbb{C}^3$ is expressed via the complex structure $J(\alpha, \beta, \gamma) = (i\alpha, i\beta, i\gamma)$, but may also be described in terms of the Hermitian scalar product

$$\langle v_1, v_2 \rangle = \alpha_1 \bar{\alpha}_2 + \beta_1 \bar{\beta}_2 + \gamma_1 \bar{\gamma}_2 = g(v_1, v_2) + i\omega(v_1, v_2) \tag{A.1}$$

We recall that a Hermitian scalar product determines a positive definite metric $g(v_1, v_2)$ and symplectic form $\omega(v_1, v_2)$ as the real and imaginary parts

of $\langle v_1, v_2\rangle$, and that these are related by $\omega(v_1, v_2) = g(v_1, Jv_2)$. The vectors $\hat{\mathcal{I}},\ \hat{\mathcal{J}},\ \hat{\mathcal{K}}$ form the "standard orthonormal basis" for $L_0 = \mathbb{R}^3$.

A Lagrangian subspace $L \subset \mathbb{C}^3$ is a real, three-dimensional subspace satisfying $\omega(v_1, v_2) = 0$ for $v_j \in L$; thus, L is *totally real* in the sense that $\langle v_1, v_2\rangle \in \mathbb{R},\ v_j \in L$. Further, L determines a g-orthogonal decomposition

$$\mathbb{C}^3 = L \oplus JL = L \oplus L^\perp \tag{A.2}$$

with summands the ± 1-eigenspaces of the corresponding real-linear reflection:

$$R_L(v_1 + Jv_2) = v_1 - Jv_2,\ v_j \in L \tag{A.3}$$

The identity $R_L Jv = -JR_L v$ holds, i.e., R_L is antiholomorphic, and it follows that R_L takes complex lines to complex lines.

All this is most transparent for L_0, the orthogonal decomposition $\mathbb{C}^3 = L_0 \oplus JL_0$, and $R_{L_0}(\alpha, \beta, \gamma) = (\bar{\alpha}, \bar{\beta}, \bar{\gamma})$. However, L_0 itself is not one of the mirrors we seek. A "real mirror" in $\mathbb{C}^3$ may be constructed directly from a given Euclidean mirror (linear 2-plane) $\mathcal{P} \subset \mathbb{R}^3$, as follows. Let $\mathcal{P}^\perp \subset \mathbb{R}^3$ denote the orthogonal complement of the given mirror. Then the vector space sum $L = \mathcal{P} \oplus i\mathcal{P}^\perp$ is a Lagrangian subspace of $\mathbb{C}^3$ with $L \cap L_0 = \mathcal{P}$. We note also that $L^\perp = JL = \mathcal{P}^\perp \oplus i\mathcal{P}$ has 1-dimensional *real part* $L^\perp \cap L_0 = \mathcal{P}^\perp$. If we define a "real mirror" to be a Lagrangian subspace $L \subset \mathbb{C}^3$ with $dim(L_0 \cap L) = 2$ and $dim(L_0 \cap JL) = 1$, then our construction sets up a *one-to-one* correspondence between such real mirrors and Euclidean mirrors $\mathcal{P} \subset \mathbb{R}^3$. In fact, it will follow from remarks below that we have thus defined a symmetric space embedding of the Grassmannian of 2-planes in $\mathbb{R}^3$ (equivalently, $\mathbb{R}P^2$ with its standard symmetric space structure) into the *Lagrangian Grassmanian* $\Lambda(3)$.

To discuss the above more concretely, consider a unitary matrix $\mathbf{U} \in U(3)$ as a transformation of $\mathbb{C}^3$ with respect to the standard basis $\hat{\mathcal{I}},\ \hat{\mathcal{J}},\ \hat{\mathcal{K}}$. Since $\mathbf{U}$ preserves the Hermitian form $\langle\ ,\ \rangle$, $\mathbf{U}$ maps one L to another. In fact, $U(3)$ acts transitively on the six dimensional homogeneous space of Lagrangian subspaces, $\Lambda(3) = U(3)/SO(3, \mathbb{R})$, known as the *Lagrangian Grassmanian*. The $U(3)$-action provides a concrete representation of reflections R_L in terms of $R_0 = R_{L_0}$. Namely, if $L = \mathbf{U}L_0 = \{\mathbf{U}a :\ a \in L_0\}$, then

$$R_L = \mathbf{U}R_0\mathbf{U}^{-1} = R_0\mathbf{U}^*\mathbf{U}^{-1} = R_0\mathbf{L} \tag{A.4}$$

Here, $\mathbf{U}^*$ denotes the complex conjugate of $\mathbf{U}$, and we have introduced the boldface letter $\mathbf{L}$ to denote the unitary matrix $\mathbf{L} = \mathbf{U}^*\mathbf{U}^{-1}$ associated with the Lagrangian subspace $L = \mathbf{U}L_0$. However, Equation A.4 must be understood in the sense of operator notation, since R_0, R_L are anti-linear operators on $\mathbb{C}^3$.

Observe that $a \in L \Leftrightarrow a = R_L a = R_0\mathbf{L}a \Leftrightarrow R_0 a = \mathbf{L}a$. Because of this relationship between L and $\mathbf{L}$, we refer to the latter as the *Schwarz matrix* associated with the Lagrangian subspace L, by direct analogy with the

Schwarz function of an analytic curve in $\mathbb{C}$, described earlier. We note that Schwarz functions are special holomorphic functions used to represent special antiholomorphic functions, via composition with complex conjugation.

With the last comment in mind, we take a moment to provide some context for the operators R_L and Schwarz matrices $\mathbf{L}$. In general, operators of the form $R = R_0\mathbf{U},\ \mathbf{U} \in U(3)$ satisfy $\langle Rv_1, Rv_2\rangle = \overline{\langle v_1, v_2\rangle}$, and make up the non-identity component of the *group of unitary/anti-unitary operators*:

$$\hat{U}(3) = U(3) \cup \{R_0\mathbf{U} : \mathbf{U} \in U(3)\} \tag{A.5}$$

Reflections $R_L \in \hat{U}(3)$ are special, since the Schwarz matrices $\mathbf{L} \in U(3)$ are. In the terminology of symmetric spaces (see [10] for the abstract theory), Schwarz matrices are *symmetric elements* g^*g^{-1} in a group-with-involution $(G, *)$; here, $G = U(3)$ and the involution is given by complex conjugation, $\mathbf{U} \leftrightarrow \mathbf{U}^*$. In this situation, one may define a symmetric space multiplication on the subset of symmetric elements by the formula: $\mathbf{L} \cdot \mathbf{M} = \mathbf{L}\mathbf{M}^{-1}\mathbf{L} = \mathbf{L}\mathbf{M}^*\mathbf{L}$.

Translating back to Lagrangian subspaces, $K = L \cdot M$ (reflection of M in L is K) defines a symmetric space multiplication on the homogeneous space $\Lambda(3)$. In this setting, the natural $U(3)$-action, $\lambda_{\mathbf{U}}L = \mathbf{U}L$, is geometrically self-evident and clearly defines a homomorphism of $U(3)$ into the group of symmetric space automorphisms $Aut(\Lambda(3))$. It is useful to note that the corresponding action on Schwarz matrices is given by *Hermitian conjugation*: $\lambda_{\mathbf{U}}\mathbf{L} = \mathbf{U}^*\mathbf{L}\mathbf{U}^{-\mathbf{1}}$.

Let us apply the above formalism to describe real mirrors and their reflections. For the first mirror $L_1 = \{p \in \mathbb{C}^3 : x, y, z \in \mathbb{R}\}$, we write $L_1 = \mathbf{U}_1 L_0$, with unitary matrix $\mathbf{U}_1$ and Schwarz matrix $\mathbf{L}_1$ given by:

$$\mathbf{U}_1 = \begin{bmatrix} \frac{1}{\sqrt{2}} & \frac{i}{\sqrt{2}} & 0 \\ \frac{1}{\sqrt{2}} & -\frac{i}{\sqrt{2}} & 0 \\ 0 & 0 & 1 \end{bmatrix}, \quad \mathbf{L}_1 = \mathbf{U}_1^*\mathbf{U}_1^{-1} = \begin{bmatrix} 0 & 1 & 0 \\ 1 & 0 & 0 \\ 0 & 0 & 1 \end{bmatrix}$$

Now observe that the matrix $\mathbf{L}_1 \in O(3, \mathbb{R}) = O(3, \mathbb{C}) \cap U(3)$ may be allowed to play more than one role. First, $R_1 = R_0\mathbf{L}_1$ gives the reflection $(\alpha, \beta, \gamma) \mapsto (\bar{\beta}, \bar{\alpha}, \bar{\gamma})$; the first mirror L_1 satisfies the (redundant) equations $\alpha = \bar{\beta},\ \beta = \bar{\alpha},\ \gamma = \bar{\gamma}$ (i.e., $x = \bar{x}, y = \bar{y}, z = \bar{z}$). Second, restriction of R_1 to L_0 is given by $\mathbf{L}_1 \in O(3)$, which may be interpreted as the matrix for reflection of $L_0 = \mathbb{R}^3$ in the 2-plane $L_1 \cap L_0 = \{(\alpha, \alpha, \gamma) : \alpha, \gamma \in \mathbb{R}\}$; namely, $(\alpha, \beta, \gamma) \mapsto (\beta, \alpha, \gamma)$.

Likewise, a general real mirror may be expressed as $L = \mathbf{M}L_1$, with $\mathbf{M} \in SO(3, \mathbb{R})$, and the corresponding Schwarz matrix $\mathbf{L} = \lambda_{\mathbf{M}}\mathbf{L}_1 = \mathbf{M}\mathbf{L}_1\mathbf{M}^{-1}$ again belongs to $O(3, \mathbb{R})$. By these two roles for $\mathbf{L}$, we recover the $1-1$ correspondence between 2-planes $\mathcal{P} \subset \mathbb{R}^3$ and real mirrors $L \subset \mathbb{C}^3$. The group of

transformations of $\mathbb{C}^3$ generated by such real mirrors is the following subgroup of $\hat{U}(3)$:

$$\hat{SO}(3,\mathbb{R}) = SO(3,\mathbb{R}) \cup \{-R_0\mathbf{M} : \mathbf{M} \in SO(3,\mathbb{R})\} \tag{A.6}$$

This group must not be confused with $O(3,\mathbb{R}) \subset O(3,\mathbb{C})$, though the two groups are abstractly isomorphic, and both act isometrically on the light cone Φ_0 with respect to the Hermitian metric in $\mathbb{C}^3$.

Acting now projectively, $\hat{SO}(3,\mathbb{R})$ may be regarded as the isometry group of Q. This is to be expected, since the metric on Q induced by the Fubini-Study metric on $\mathbb{C}P^2$ was seen, in the previous section, to make Q isometric to the standard sphere of radius *one*. Then real mirrors are to Q as planes through the origin are to S^2—generators of the full isometry group.

In either case, a reflection has fixed point set consisting of a geodesic; this is obvious for S^2 and for Q follows by the simple geometric argument used in the proof of Proposition 9.1. While a geodesic in S^2 is the intersection of S^2 with a plane, a real mirror in $\mathbb{C}^3$ has to be considered projectively in order to be intersected with Q. If this seems imperfectly parallel to the situation for S^2, we note that the projectivized real mirror may be described more intrinsically as a *Lagrangian real projective plane*; it is a special Lagrangian submanifold of $\mathbb{C}P^2$ which is topologically $\mathbb{R}P^2$. The most familiar example, of course, is the usual real x, y-plane (appropriately compactified).

Appendix B. Equivariant parameterization of the quadric

The standard quadric Q has a *standard parameterization* . Actually, we will use this term to refer to either of two maps, $\psi : \mathbb{C}P^1 \to Q$ or $\varphi : S^2 \to Q$, depending on whether we wish to regard $\mathbb{C}P^1$ or S^2 as the domain of the parameterization . Either way, the parameterization deserves to be called "standard" because it is equivariant with respect to the relevant group actions in domain and range. This key property is inherited from corresponding results for related 3-dimensional spaces, which we consider first.

The *standard parameterization* of the light cone $\Psi : \mathbb{C}^2 \to \Phi_0$ is given by:

$$(\mu,\nu) \overset{\Psi}{\longmapsto} (\alpha,\beta,\gamma) = (\mu^2 - \nu^2, i(\mu^2+\nu^2), -2\mu\nu) \tag{B.1}$$

Some features of Ψ follow trivially from the formula. For $(\mu,\nu) \in \mathbb{C}^2$, $w = \Psi(\mu,\nu)$ satisfies $w \cdot w = 0$. Conversely, if $w = (\alpha,\beta,\gamma) \in \mathbb{C}^3$ satisfies $w \cdot w = 0$ $(w \neq (0,0,0))$, there are exactly two solutions $\pm(\mu,\nu)$ to the system

$$\mu^2 = \frac{\alpha - i\beta}{2}, \quad \nu^2 = -\frac{\alpha + i\beta}{2}, \quad \mu\nu = -\frac{\gamma}{2}.$$

Further, $\mu\bar{\mu}+\nu\bar{\nu}=1$ precisely when $w=\Psi(\mu,\nu)$ satisfies $\langle w,w\rangle=2$. Thus, by restricting Ψ to S^3 and normalizing, we obtain a double covering $\hat{\Psi}=\frac{1}{\sqrt{2}}\Psi:S^3\to\mathbb{R}P^3$, which is explicitly invertible, locally, via extraction of square roots.

On the other hand, points in the light cone may be represented in terms of certain pairs of real 3-vectors. To any pair of real vectors $p,q\in L_0$, we may associate the complex vector $w=p+iq\in\mathbb{C}^3$. Any complex vector $w\in\mathbb{C}^3$ may be so represented in terms of its *real* and *imaginary parts*, $p=Re[w],\ q=Im[w]\in L_0$. Thus, the fundamental and Hermitian forms may be expressed: $w\cdot w=p\cdot p-q\cdot q+2ip\cdot q$ and $\langle w,w\rangle=p\cdot p+q\cdot q$. The first equation shows that w belongs to the light cone $\Phi_0=\Phi^{-1}(0)$ if and only if p,q are perpendicular and of equal length. In this case, p and q are unit vectors exactly when the normalized vector $v=\frac{1}{\sqrt{2}}(p+iq)$ belongs to the 5-sphere $S^5\subset\mathbb{C}^3$. Thus, the $1-1$ correspondence $(p,q)\leftrightarrow v$ satisfies:

$$p,q\in L_0 \text{ are orthonormal} \Leftrightarrow v=\frac{1}{\sqrt{2}}(p+iq)\in\Phi_0\cap S^5\approx\mathbb{R}P^3 \qquad \text{(B.2)}$$

Here, $\Phi_0\cap S^5\approx\mathbb{R}P^3$ denotes topological equivalence, to be described presently.

Using the basis $\hat{\mathcal{I}},\ \hat{\mathcal{J}},\ \hat{\mathcal{K}}$, the orthonormal vectors $p,q,r=p\times q$ form the columns of a rotation matrix $\mathbf{M}\in SO(3)\approx\mathbb{R}P^3$. Thus, the above correspondence implies $\Phi_0\cap S^5\approx SO(3)$. But the homeomorphism $SO(3)\approx\mathbb{R}P^3$ is well-known, e.g., as a byproduct of the spinor theory of rotations. That is, the special unitary group $SU(2)$ is topologically the three sphere S^3, and the adjoint representation $\mathrm{Ad}:SU(2)\to SO(3)$ is a double cover which identifies antipodal points of S^3. To summarize, Equation B.2 defines an embedding

$$\tau:SO(3)\to\mathbb{R}P^3\subset\mathbb{C}^3,$$

where the notational shorthand $\mathbb{R}P^3=\Phi_0\cap S^5$ is understood. The role of τ will be more fully explained after we recall formulas for the adjoint representation.

Let us begin by recalling the adjoint action of the special linear group $SL(2,\mathbb{C})$ on its Lie algebra $sl(2,\mathbb{C})\simeq\mathbb{C}^3$. Elements of the former will be written $\mathbf{m}=\begin{bmatrix}a & b\\ c & d\end{bmatrix}$ with $\det(\mathbf{m})=ad-bc=1$. The latter may be identified with the space of traceless, 2×2 complex matrices, $sl(2,\mathbb{C})\simeq\{\mathbf{X}=A\mathbf{e}_1+B\mathbf{e}_2+C\mathbf{e}_3:A,B,C\in\mathbb{C}\}$. Here we are using the basis of Pauli matrices:

$$\mathbf{e}_1=\begin{bmatrix}0 & 1\\ 1 & 0\end{bmatrix},\quad \mathbf{e}_2=\begin{bmatrix}0 & -i\\ i & 0\end{bmatrix},\quad \mathbf{e}_3=\begin{bmatrix}1 & 0\\ 0 & -1\end{bmatrix}$$

The adjoint action is given by conjugation: $\mathrm{Ad}_{\mathbf{m}}\mathbf{X}=\mathbf{m}\mathbf{X}\mathbf{m}^{-1}$. Note $\mathbf{X}\in sl(2,\mathbb{C})\Rightarrow\mathrm{Ad}_{\mathbf{m}}\mathbf{X}\in sl(2,\mathbb{C})$ (since $\mathrm{tr}(\mathbf{m}\mathbf{X}\mathbf{m}^{-1})=\mathrm{tr}(\mathbf{m}^{-1}\mathbf{m}\mathbf{X})=\mathrm{tr}(\mathbf{X})$) and Ad defines a linear action on $sl(2,\mathbb{C})$.

In fact, $\mathrm{Ad}_{\mathbf{m}}\mathrm{Ad}_{\mathbf{n}} = \mathrm{Ad}_{\mathbf{mn}}$, and Ad defines a homomorphism onto a subgroup of $GL(3,\mathbb{C})$, which may be identified as follows. Consider the bilinear form $(\mathbf{X},\mathbf{Y}) = \frac{1}{2}\mathrm{Tr}(\mathbf{XY})$ on $sl(2,\mathbb{C})$; note that it agrees with the fundamental form $\Phi(\mathbf{X}) = (\mathbf{X},\mathbf{X})$ on $\mathbb{C}^3$. Since $(\ ,\ )$ is Ad-invariant ($(\mathrm{Ad}_g\mathbf{X}, \mathrm{Ad}_g\mathbf{Y}) = \frac{1}{2}\mathrm{Tr}(g\mathbf{X}g^{-1}g\mathbf{Y}g^{-1}) = \frac{1}{2}\mathrm{Tr}(\mathbf{XY}) = (\mathbf{X},\mathbf{Y})$), it follows that $\mathrm{Ad}_g \in SO(3,\mathbb{C})$. In fact, $\mathrm{Ad} : SL(2,\mathbb{C}) \to SO(3,\mathbb{C})$ defines a homomorphism whose kernel may be shown to be $\{\pm\mathbf{Id}\}$.

To be explicit, the matrix representing $\mathrm{Ad}_{\mathbf{m}}$ with respect to the Pauli basis is:

$$\mathbf{M} = \begin{bmatrix} \frac{1}{2}(a^2-b^2-c^2+d^2) & \frac{-i}{2}(a^2+b^2-c^2-d^2) & -ab+cd \\ \frac{i}{2}(a^2-b^2+c^2-d^2) & \frac{1}{2}(a^2+b^2+c^2+d^2) & -i(ab+cd) \\ -ac+bd & i(ac+bd) & ad+bc \end{bmatrix} \tag{B.3}$$

With $ad-bc=1$, the given matrix satisfies $\mathbf{MM}^T = \mathbf{M}^T\mathbf{M} = \mathbf{Id}$, i.e., $\mathbf{M} \in SO(3,\mathbb{C})$.

Remark B.1. We have taken the time to recall $\mathrm{Ad} : SL(2,\mathbb{C}) \to SO(3,\mathbb{C})$ because we view it as the "source" of most of the relevant symmetry and equivariance properties, as will be seen below. For the moment, we note that it is now easy to see why the symmetry group of a quadric is the Möbius group. We have already discussed the symmetry group of the standard quadric, $Sym(Q) = SO(3,\mathbb{C})$, and the last paragraph gives the identification with the Möbius group $PSL(2,\mathbb{C}) \simeq SL(2,\mathbb{C})/\{\pm\mathbf{Id}\} \simeq SO(3,\mathbb{C})$. Since any (irreducible) quadric C is projectively equivalent to Q, it follows that $Sym(C) \simeq PSL(2,\mathbb{C})$.

Restriction of Ad gives the famous "spinor map" $\mathrm{Ad} : SU(2) \to SO(3,\mathbb{R})$. Writing $\mathbf{m} \in SU(2)$ as $\mathbf{m} = \begin{bmatrix} \mu & -\bar{\nu} \\ \nu & \bar{\mu} \end{bmatrix}$, $\mu\bar{\mu}+\nu\bar{\nu}=1$, Equation B.3 specializes as follows:

$$\mathbf{M} = \begin{bmatrix} \mathbf{Re}[\mu^2-\nu^2] & \mathbf{Im}[\mu^2-\nu^2] & \mathbf{Re}[2\bar{\mu}\nu] \\ \mathbf{Re}[i(\mu^2+\nu^2)] & \mathbf{Im}[i(\mu^2+\nu^2)] & \mathbf{Im}[2\bar{\mu}\nu] \\ \mathbf{Re}[-2\mu\nu] & \mathbf{Im}[-2\mu\nu] & |\mu|^2-|\nu|^2 \end{bmatrix} \tag{B.4}$$

The columns of $\mathbf{M} = [p\ q\ r]$ are, of necessity, orthonormal and $p \times q = r$. We express $\mathbf{M}$ in this particular form to make the following observations:

- *The first two columns are, respectively, the real and imaginary parts of the isotropic vector* $w = p+iq = \Psi(\mu,\nu) \in \Phi_0$*; normalizing,* $v = \frac{1}{\sqrt{2}}(p+iq) \in \mathbb{R}P^3 = \Phi_0 \cap S^5$.
- *The third column maps to* $\pi_{sp}(r) = \nu/\mu$ *by stereographic projection* $\pi_{sp} : S^2 \to \mathbb{C}$ *from the south pole.*

The second observation (which will play a role later) follows by a simple computation from $\pi_{sp}(r) = \pi_{sp}(a,b,c) = \frac{a+ib}{1+c}$. The first observation, which is self-evident, easily gives an important conclusion. Note that $\mathbf{m} \in SU(2)$ may be identified with its first column $\mathbf{u} = \begin{bmatrix}\mu\\ \nu\end{bmatrix}$, which may be regarded as an element of S^3. With this understanding, we have the factorization $\hat{\Psi} = \tau \circ \mathrm{Ad}$. Then the equivariance property of $\hat{\Psi}$,

$$\hat{\Psi}(\mathbf{nu}) = \mathrm{Ad}_{\mathbf{n}}\hat{\Psi}(\mathbf{u}), \quad \mathbf{n} \in SU(2), \quad \mathbf{u} \in S^3, \tag{B.5}$$

follows from corresponding properties of the factors $\tau,\ \mathrm{Ad}$.

Let us now bring projective geometry back into the mix. $\Psi : \mathbb{C}^2 \to \mathbb{C}^3$ takes complex lines to complex lines, so Ψ induces a projective space mapping $\psi : \mathbb{C}P^1 \to \mathbb{C}P^2$. (Re-interpret Equation B.1, replacing Ψ by ψ and using homogeneous coordinates on $\mathbb{C}P^1$ and $\mathbb{C}P^2$.) Equivalently, ψ is induced by $\hat{\Psi} : S^3 \to S^5$. Recall, the circle group $U(1) = \{e^{i\theta}\}$ acts on $S^{2n+1} \subset \mathbb{C}^{n+1}$ via multiplication of components by $e^{i\theta}$, and the Hopf projection $\pi : S^{2n+1} \to \mathbb{C}P^n$ identifies points of the same circle-orbit. The sphere S^{2n+1} is thus pictured as a union of circles (*bundle of fibers*), one for each point in $\mathbb{C}P^n$. (S^{2n+1} is in fact a *principal* $U(1)$*-bundle.*) Now observe that $\hat{\Psi}$ relates the circle actions on S^3 and S^5 according to $\hat{\Psi}(\mathbf{u}e^{i\theta}) = \hat{\Psi}(\mathbf{u})e^{i2\theta},\ \mathbf{u} \in S^3$; that is, Hopf fibers in S^3 doubly-cover their image fibers in S^5. Thus, the double covering $\hat{\Psi} : S^3 \to \mathbb{R}P^3 \subset S^5$ yields an injection $\psi : \mathbb{C}P^1 \to \mathbb{C}P^2$.

At this point one may refer to Figure 11 for the inter-relationships and equivariance properties of the various maps of interest. After a few further remarks, the diagram should be self-explanatory (we omit details). Regarding vertical arrows: Aside from Hopf projections π, we use the *third column projection* $\pi(\mathbf{M}) = \pi([p\ q\ r]) = r$. On bottom: The Riemann sphere parameterization $r = \rho(\mu/\nu) = (a,b,c)$ is the one required to complete the outer rectangle in the commutative diagram; it is the inverse of $r \mapsto \frac{\mu}{\nu} = \frac{1}{\pi_{sp}(r)} = \frac{1+c}{a+ib}$. (To verify, use the second observation after Equation B.4).

Of primary interest are the maps ψ and $\varphi = \psi \circ \rho^{-1}$; either may be called *the standard parameterization of* Q (but it will be seen that they admit quite different descriptions). Like all other "non-vertical maps" in the diagram, ψ and φ are equivariant with respect to the relevant group actions. For example, note that the circle actions on S^3 and S^5 commute with the respective $SU(2)$ and $SU(3)$ actions on these spheres. It follows that the induced actions on $\mathbb{C}P^1$ and $\mathbb{C}P^2$ are intertwined by $\psi : \mathbb{C}P^1 \to \mathbb{C}P^2$—see the *left trapezoid* in the diagram. That is, Equation B.5 holds, with ψ substituted for $\hat{\Psi}$ and $\mathbb{C}P^1$ in place of S^3.

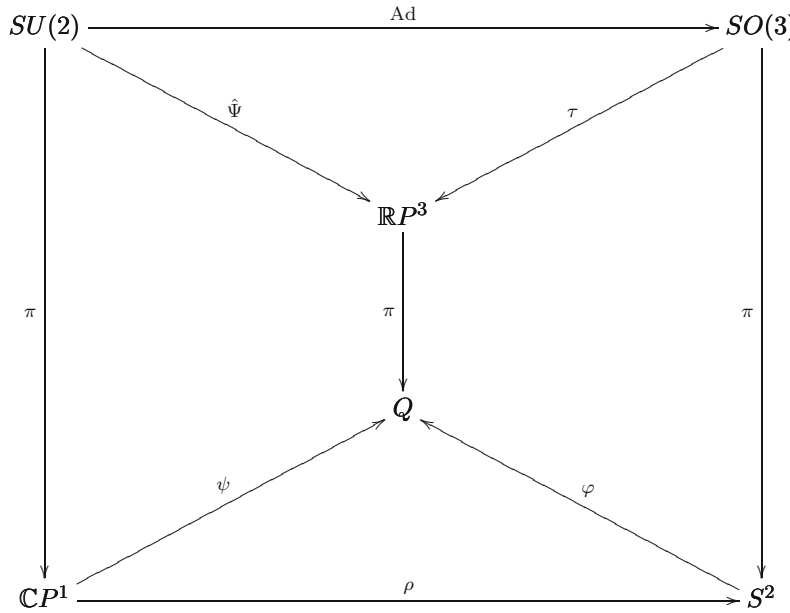

FIGURE 11. Equivariant mappings (non-vertical arrows).

Likewise, equivariance of φ is best explained via the *right trapezoid*. Namely, φ can be described as follows. Given $r \in S^2$, choose p, q to complete an orthonormal frame $\mathbf{M} = [p\, q\, r] \in SO(3)$, and note that $\pi(\tau(\mathbf{M})) = [p+iq] \in Q$ is independent of the choice just made. Thus, $r \overset{\varphi}{\mapsto} [p + iq]$ is not only well-defined, it is also obviously equivariant with respect to the $SO(3, \mathbb{R})$ actions on S^2 and Q. Finally, Proposition 8.1 now follows by extension to orientation-reversing symmetries, as explained in Section 8.

Appendix C. Two *Mathematica* animations

C.1. Manipulation of Joukowski airfoil

The following *Mathematica* code creates a *manipulate* window with two sliders. As one varies the center and radius of a circle C with these sliders, one sees what happens to the image "airfoil" $j_+(C)$.

```
j[z_] = (z + 1/z)/2;

c[t_, z_, r_] = r Exp[I t] + z;

jofc[z_, r_]:= ParametricPlot[{Re[j[c[t, z, r]]], Im[j[c[t, z, r]]]},
                    {t, 0, 2 Pi}, PlotRange -> {{-2, 2}, {-2, 2}},
               Axes -> False, PlotStyle -> {Thickness[.006], Blue}];
```

```
circ[c_, r_] = Graphics[{Red, Thickness[.002], Circle[c, r]}];

points = Graphics[{PointSize[.015], Point[{{-1, 0}, {1, 0}}]}];

z[{x_, y_}] = x + I y;

Manipulate[Show[jofc[z[xy], r], circ[xy, r], points],
 {xy, {0, 0}, {3, 1}}, {r, .5, 3}]
```

C.2. Animation of the Watt linkage

The following animation shows how a lemniscate is traced out by the midpoint of a three-rod linkage, as the upper rod pivots at a constant rate.

```
cplus[t_] = Sqrt[2] Exp[I t] + I; cminus[t_] = -1/cplus[t];
lemniscate[t_] = (cplus[t] + cminus[t])/2; xy[z_] = {Re[z], Im[z]};

plot8 = ParametricPlot[xy[lemniscate[t]], {t, -Pi, Pi},
             PlotRange -> {{-2, 2}, {-5/2, 5/2}}, Axes -> False,
             PlotStyle -> {Thickness[.005], Blue}];

rods[t_] = Graphics[{Thickness[.005], Line[{{{0, 1}, xy[cplus[t]]},
         {{0, -1}, xy[cminus[t]]}, {xy[cplus[t]], xy[cminus[t]]}}]}];

joints[t_] = Graphics[{EdgeForm[Thick], FaceForm[White],
                   Disk[xy[cplus[t]], .04], Disk[xy[cminus[t]], .04],
                   Disk[{0, 1}, .04], Disk[{0, -1}, .04],
                   FaceForm[Red], Disk[xy[lemniscate[t]], .05]}];

circles = Graphics[{Thickness[.0027], Circle[{0, 1}, Sqrt[2]],
               Circle[{0, -1}, Sqrt[2]], Circle[{0, 0}, 1]}];

Watthinge[t_] := Show[plot8, circles, rods[t], joints[t]]
Animate[Watthinge[t], {t, 0, 2 Pi}]
```

References

[1] A.B. Basset, *An Elementary Treatise on Cubic and Quartic Curves*, Merchant Books, 2007. (original copyright, 1901)

[2] E. Brieskorn and H. Knörrer, *Plane Algebraic Curves*, Birkhäuser, 1986.

[3] Annalisa Calini and Joel Langer, *Schwarz reflection geometry I: continuous iteration of reflection*, Math. Z., **244** (2003), pp. 775–804.

[4] Philip J. Davis, *The Schwarz Function and its Applications*, The Carus Mathematical Monographs, No. 17, The Mathematical Association of America, 1974.

[5] H. Hilton, *Plane Algebraic Curves, second edition*, London, Oxford University Press, 1932.

[6] G. Jones and D. Singerman, *Complex Functions an algebraic and geometric viewpoint*, Cambridge University Press, 1997.

[7] Felix Klein, *The icosahdron and the solution of equations of the fifth degree*, Dover Publications, 1956.

[8] Joel Langer and David Singer, *Foci and foliations of real algebraic curves*, Milan J. Math., **75** (2007) No. 1, pp. 225–271.

[9] ———, *When is a curve an octahedron?*, Amer. Math. Monthly (to appear).

[10] Ottmar Loos, *Symmetric Spaces I: General Theory*, W. A. Benjamin, Inc. (1969).

[11] Linda Ness, Curvature on algebraic plane curves. I, Compositio Mathematica, **35** (1977), pp. 57–63.

[12] Victor Prasolov and Yuri Solovyev, *Elliptic Functions and Elliptic Integrals*, Translations of Mathematical Monographs, Vol. 170, 1997. American Mathematical Society.

[13] M. Rosen, *Abel's theorem on the lemniscate*, Amer. Math. Monthly, **88** (1981), pp. 387–395.

[14] George Salmon, *A Treatise on the Higher Plane Curves, Third Edition*, G. E. Stechert & Co., New York, 1934.

[15] J. Stillwell, *Mathematics and Its History*, 2nd ed., Springer, 2002.

[16] C. Zwikker, *The Advanced Geometry of Plane Curves and their Applications*, Dover Publications, 1963.

Joel C. Langer and David A. Singer
Department of Mathematics
Case Western Reserve University
Cleveland, OH 44106-7058
USA
e-mail: joel.langer@case.edu
david.singer@case.edu

Received: January 21, 2010.